T.C.

BAHCESEHIR UNIVERSITY

GRADUATE SCHOOL

THE DEPARTMENT OF NEUROSCIENCE

THE IMPACT OF HYDROGEN PEROXIDE AND TUMOR NECROSIS FACTOR-ALPHA ON THE VIABILITY OF DIFFERENT HUMAN GLIOMA CELL LINES

MASTER'S THESIS

REZVAN MOHAMMADI

ISTANBUL 2024

T.C.

BAHCESEHIR UNIVERSITY

GRADUATE SCHOOL OF EDUCATION

THE DEPARTMENT OF NEUROSCIENCE

THE IMPACT OF HYDROGEN PEROXIDE AND TUMOR NECROSIS FACTOR-ALPHA ON THE VIABILITY OF DIFFERENT HUMAN GLIOMA CELL LINES

MASTER'S THESIS

REZVAN MOHAMMADI

THESIS ADVISOR

ASSIST. PROF. DR. MEHMET OZANSOY

ISTANBUL 2024

T.C.

BAHCESEHIR UNIVERSITY

GRADUATE SCHOOL

MASTER THESIS APPROVAL FORM

Program Name:	Neuroscience
Student's Name and Surname:	Rezvan Mohammadi
Name Of The Thesis:	The Impact of Hydrogen Peroxide and Tumor Necrosis factor-alpha On the Viability of Different Human Glioma Cell Lines
Thesis Defense Date:	02/09/2024

This thesis has been approved by the Graduate School which has fulfilled the necessary conditions as Master thesis.

Assoc.Prof. Yücel Batu SALMAN

Institute Director

This thesis was read by us, quality and content as a Master's thesis has been seen and accepted as sufficient.

	Title/Name	**Institution**	**Signature**
Thesis Advisor's	Asist.Prof.Dr.Mehmet Ozansoy	Istanbul Medipol University	
Member's	Asist.Prof.Dr. Timuçin	Bahçeşehir University	

Member's	Asist.Prof.Dr.Yeşim Neğiş	Bahçeşehir University	

I hereby declare that all information in this document has been obtained and presented in accordance with academic rules and ethical conduct. I also declare that, as required by these rules and conduct, I have fully cited and referenced all material and results that are not original to this work.

Name, Last Name: Rezvan Mohammadi

Signature:

ABSTRACT

THE IMPACT OF HYDROGEN PEROXIDE AND TUMOR NECROSIS FACTOR-ALPHA ON THE VIABILITY OF DIFFERENT HUMAN GLIOMA CELL LINES

Rezvan, Mohammadi

Master's Program in Neuroscience

Supervisor: Assist. Prof. Dr. Mehmet Ozansoy

October 2024, 87 pages

Gliomas, particularly glioblastomas, represent one of the most challenging types of brain tumors due to their aggressive nature and resistance to conventional treatments. This study investigates the effects of hydrogen peroxide (H_2O_2) and tumor necrosis factor-alpha (TNF-α) on the viability of various human glioma cell lines. By examining the differential responses of these cell lines to oxidative stress and inflammatory cytokines, the research seeks to provide deeper insights into potential therapeutic strategies that leverage these pathways. The findings could pave the way for novel treatments that improve patient outcomes in glioma management

Key Words: Glioma, Glioblastoma, Hydrogen Peroxide (H_2O_2), Tumor Necrosis Factor Alpha (TNF-α), Oxidative stress (ROS)

ÖZ

HİDROJEN PEROKSİT VE TÜMÖR NEKROZ FAKTÖRÜ-ALFA'NIN FARKLI İNSAN GLİOMA HÜCRE HATLARININ CANLILIĞI ÜZERİNDEKİ ETKİSİ

Rezvan, Mohammadi
Nörobilim Yüksek Lisans Programı
Tez Danışmanı: Asistan. Doç. Dr. Mehmet Ozansoy

Ekim 2024, 87 sayfa

Gliomlar, özellikle glioblastomalar, agresif doğaları ve geleneksel tedavilere dirençleri nedeniyle en zorlu beyin tümörü türlerinden birini temsil eder. Bu çalışma, çeşitli insan glioma hücre hatlarının yaşama oranı üzerindeki hidrojen peroksit (H_2O_2) ve tümör nekroz faktörü-alfa (TNF-α) etkilerini araştırmaktadır. Bu hücre hatlarının oksidatif strese ve inflamatuar sitokinlere karşı farklı tepkilerini inceleyerek, bu yolları kullanarak potansiyel terapötik stratejiler hakkında daha derin bilgiler sağlamayı amaçlamaktadır. Bulgular, glioma yönetiminde hasta sonuçlarını iyileştiren yeni tedavilerin önünü açabilir.

Anahtar Kelimeler: Glioma, Glioblastoma, Hidrojen Peroksit (H_2O_2), Tümör Nekroz Faktörü Alfa (TNF-α), Oxidatif stres (ROS)

Dedicating

ACKNOWLEDGEMENTS

Sydney J. Harris once said, "The whole purpose of research is to turn mirrors into windows." My academic journey has been a thrilling and comprehensive adventure, and I am deeply thankful to everyone who supported me in this the way.

First and foremost, I am profoundly grateful to GOD, the Almighty, for providing opportunities to learn, granting me patience and strength, and making this journey smoother. My heartfelt thanks also go to my supervisor, Assist. Prof. Dr. MEHMET OZANSOY. His wisdom and guidance have been crucial in shaping my research, helping me ask the right questions, and bolstering my confidence even when I doubted myself. He has emphasized that intellectual curiosity is the foundation of success. His mentorship has helped me recognize my potential and set goals for both academic and personal growth.

I also extend my sincere appreciation to our program advisor, Doç. Dr. TIMUÇIN AVŞAR, for his constant assistance and eagerness to share his knowledge, as well as for providing the necessary equipment for this project.

My gratitude goes to my lab colleagues Bervis and Baris for their support, motivation, and kindness. Being part of this team is an honor, and I wish each of them the very best.

Finally, my family back home deserves my utmost thanks. They are my greatest support and blessing. My parents, siblings (Amin, Payman), and friends have surrounded me with love, care, and prayers. Their unwavering support has been invaluable.

TABLE OF CONTENTS

LIST OF TABLES

TABLES

LIST OF FIGURES

FIGURES

LIST OF ABBREVIATIONS

LGGs	Low Grade Gliomas
HGGs	High Grade Gliomas
GBM	Glioblastoma
H_2O_2	Hydrogen Peroxide
NO	Nitric Oxide
SOD	Superoxide Dismutase
EGFR	Epidermal Growth Factor Receptor
RTK	Receptor Tyrosine Kinase
MAPK	Mitogen-activated Protein Kinase
ETC	Electron Transport Chain
ATP	Adenosine Triphosphate
ROS	Reactive Oxygen Species
OS	Oxidative Stress
SOD1	Superoxide Dismutase1
DNA	Deoxyribonucleic Acid
GPCR	G-Protein Coupled Receptor
GLUT-4	Glucose Transporter-4
PI3K	Phosphatidylinositol-3-kinase
Akt	Protein Kinase
CREB	cAMP-response Element Binding Protein
APE1	Apurinic/Apyrimidinic Endonuclease 1
CPD3B	Cyclic Nucleotide Phosphodiesterase 3B
PIP2	Phosphoinositol Bisphosphate
PDK1	Pyruvate Dehydrogenase Kinase
GSK3β	Glycogen Synthase Kinase 3β
Ras/Raf	Small Protein GTPases
Grb2	Growth Factor Receptor-bound Protein
AC	Adenyl Cyclase
cAMP	Cyclic AMP
PKA	Protein Kinase A
TDP-43	Tar DNA-binding Protein 43

ODC	Oligodendrocyte
MBP	Myelin Basic Protein
PLP	Myelin Proteolipid Protein
TNF-α	Tumor Necrosis Factorα
IL-6	Interleukin-6
PDGFRA	Platelet Derived Growth Factor Receptor Alpha
MEK/ERK	MAPK Kinase/Extracellular Signal Regulated Kinase
mTOR	Mammalian Target of Rapamycin
CDK4	Cyclin Dependent Kinase 4
NF-$_k$B	Nuclear Factor Kappa Light Chain Enhancer of Activated B Cells
DISC	Death Inducing Signaling Complex
RIPK1	Receptor Interacting Protein Kinas 1
JAK/STAT	Janus kinase/Signal Transducers and Activators of Transcription

Chapter 1

Introduction

1.1 Theoretical Overview

Gliomas are the most common type of primary brain tumors, originating from glial cells that support and protect neurons in the central nervous system. Among gliomas, glioblastomas (GBM) are the most aggressive and have the poorest prognosis. Despite advances in surgical techniques, radiotherapy, and chemotherapy, the median survival time for patients with glioblastoma remains dismal, often less than 15 months (Stupp et al., 2005). The inherent heterogeneity and adaptability of glioma cells contribute significantly to their resistance to treatment, necessitating a multifaceted approach to better understand and combat these tumors.

1.2 Statement of the Problem

The problem addressed by this study is the limited effectiveness of current treatments for glioblastoma, which is characterized by rapid proliferation, extensive infiltration, and resistance to conventional therapies. There is a critical need for new therapeutic strategies that can overcome these challenges. Understanding the effects of hydrogen peroxide and tumor necrosis factor-alpha on glioma cell viability may reveal novel approaches to enhance treatment efficacy and improve patient outcomes.

1.3 Purpose of The Study

The purpose of this study is to elucidate the effects of H_2O_2 and TNF-α on the viability of different human glioma cell lines, both independently and in combination. By uncovering potential combined interactions between these agents, the research aims to identify new therapeutic strategies that could be more effective than current treatments. The significance of this study lies in its potential to contribute to the development of targeted therapies that exploit the vulnerabilities of glioma cells to

oxidative stress and inflammatory signalling. Such therapies could significantly improve the prognosis and quality of life for patients with gliomas.

1.4 Research Questions

1.What concentrations of hydrogen peroxide (H_2O_2) significantly affect the survival rates of various human glioma cell lines?

2. How does tumor necrosis factor-alpha (TNF-α) influence the pro-apoptotic and necroptotic pathways in glioma cells, and what impact does this have on their viability?

3. What are the combined effects of H_2O_2 and TNF-α on glioma cell viability, and can this combination serve as a potential new therapeutic strategy?

4. What molecular mechanisms are involved in the response of glioma cells to H_2O_2 and TNF-α, particularly concerning NF-κB, MAPK, and apoptotic pathways?

5. How can oxidative stress and inflammatory signalling be leveraged to develop targeted therapies for glioma treatment?

1.5 Significance of the Study

- This study will expand the understanding of oxidative stress in glioma cells, potentially revealing new pathways and mechanisms that influence cell survival.
- By exploring TNF-α's role in glioma cell death, the research may identify novel therapeutic targets for pro-apoptotic and necroptotic induction in glioma treatment.
- Combination therapy using H_2O_2 and TNF-α could offer insights into more effective glioma treatment strategies, which may improve patient outcomes.
- Identifying the molecular mechanisms, including key signalling pathways, will help pinpoint crucial regulatory steps in glioma cell death, potentially leading to new interventions.
- The findings could contribute to the development of targeted therapies that harness oxidative stress and inflammation modulation to combat glioma, addressing a pressing need for more effective treatment options.

1.6 Limitations of the Study

- Cell Line Variability: Results obtained from different glioma cell lines may not be directly applicable to all gliomas, given the heterogeneity of tumor types.
- In Vitro Nature: The experiments will be conducted at the cell culture level, which may not fully mimic the in vivo tumor environment and its complexities.
- Concentration Thresholds: Finding the precise concentration of H_2O_2 and TNF-α that can induce significant cell death without excessive toxicity may be challenging.
- Molecular Pathways: The study may be limited by the ability to comprehensively analyze all molecular pathways involved in the cellular response to oxidative stress and TNF-α.
- Translation to Clinical Application: While this research may provide foundational knowledge, translating these findings into clinical therapies will require further extensive in vivo and clinical trials.

1.7 Definitions

- Hydrogen Peroxide (H_2O_2): A reactive oxygen species that can induce oxidative stress in cells, potentially leading to cell damage or death.
- Tumor Necrosis Factor-Alpha (TNF-α): A cytokine involved in systemic inflammation that can promote cell death through apoptotic and necroptotic pathways.
- Glioma: A type of tumor originating from glial cells in the brain or spine, known for its aggressive nature and resistance to conventional therapies.
- Oxidative Stress: An imbalance between the production of reactive oxygen species (such as H_2O_2) and the body's ability to detoxify them, often resulting in cellular damage.
- Apoptosis: A form of programmed cell death that occurs in a regulated manner, often as a defense mechanism against cancerous changes in cells.
- Necroptosis: A form of programmed necrosis or inflammatory cell death, distinct from apoptosis, which can be triggered by specific signals like TNF-α.

- NF-κB Pathway: A critical signalling pathway involved in inflammatory responses, cell proliferation, and survival, which may influence glioma cell responses to stress.
- MAPK Pathway: A signalling pathway that plays a role in cell growth, differentiation, and apoptosis, potentially affected by oxidative stress and cytokine signalling.
- Targeted Therapy: Treatment that specifically targets molecular pathways or mechanisms in cancer cells, aiming to minimize damage to normal cells.

Chapter 2

Literature Review

2.1 Introduction

Gliomas constitute approximately 30% of all brain and central nervous system tumors and 80% of all malignant brain tumors. These tumors originate from glial cells, including astrocytes, oligodendrocytes, and ependymal cells. The World Health Organization (WHO) classifies gliomas into four grades based on their histological features, with grade I and II being low-grade gliomas and grade III and IV being high-grade gliomas (Louis et al., 2016).

Low-grade gliomas (LGGs) include pilocytic astrocytoma (grade I) and diffuse astrocytoma (grade II). These tumors are less aggressive, with slower growth rates and better prognosis compared to high-grade gliomas. However, LGGs can progress to higher-grade malignancies over time, necessitating careful monitoring and management (Louis et al., 2016).

High-grade gliomas (HGGs) include anaplastic astrocytoma (grade III) and glioblastomas (grade IV). These tumors are characterized by rapid proliferation, significant invasiveness, and a propensity for resistance to conventional therapies. Glioblastoma, the most aggressive form, accounts for nearly 50% of all gliomas and is associated with a median survival time of approximately 15 months despite aggressive treatment (Stupp et al., 2005).

2.2 Molecular Pathways in Glioma Development and Progression

The development and progression of gliomas are driven by a complex interplay of genetic and epigenetic alterations that disrupt normal cellular functions. Key molecular pathways involved in glioma pathogenesis include:

2.2.1 Receptor tyrosine kinase (RTK)/RAS/PI3K pathway. Mutations and amplifications in genes encoding receptor tyrosine kinases (RTKs) such as EGFR, PDGFRA, and MET is common in gliomas. These alterations lead to the activation of downstream signaling pathways, including the RAS/RAF/MEK/ERK and

PI3K/AKT/mTOR pathways, which promote cell proliferation, survival, and angiogenesis (Cancer Genome Atlas Research Network, 2008).

2.2.2 P53 pathway. The tumor suppressor p53 plays a crucial role in regulating cell cycle arrest, apoptosis, and DNA repair. Mutations in the TP53 gene are frequently observed in gliomas, leading to the loss of p53 function and contributing to uncontrolled cell growth and resistance to apoptosis (Zhu et al., 2012).

2.2.3 RB pathway. The retinoblastoma (RB) protein is another critical tumor suppressor involved in cell cycle regulation. Alterations in the RB pathway, including mutations in the RB1 gene and the amplification of CDK4 and CDK6, are common in gliomas and contribute to aberrant cell cycle progression and tumorigenesis (Inda et al., 2010).

2.3 Oxidative Stress and Cancer

Oxidative stress, characterized by an imbalance between the production of reactive oxygen species (ROS) and the cell's antioxidant defenses, plays a dual role in cancer biology. At low levels, ROS are involved in cellular signaling and homeostasis, but at high levels, they cause significant damage to cellular components, leading to cell death (Trachootham et al., 2009).

2.4 ROS and Cancer Initiation

ROS can cause DNA damage, leading to mutations and genomic instability, which are hallmarks of cancer initiation. The oxidative damage to DNA includes base modifications, single and double-strand breaks, and the formation of DNA adducts, which, if not properly repaired, can result in carcinogenesis (Sosa et al., 2013).

2.5 ROS and Cancer Progression

In established tumors, cancer cells often exhibit increased ROS levels, which promote tumor progression by enhancing cell proliferation, survival, angiogenesis, and

metastasis. Cancer cells adapt to high ROS levels by upregulating antioxidant defences, such as glutathione, superoxide dismutase, and catalase, to maintain redox homeostasis (Gorrini et al., 2013).

2.6 Therapeutic Targeting of ROS

The differential redox status between cancer cells and normal cells provides a therapeutic window for selectively targeting cancer cells with ROS-inducing agents. For instance, treatments that further increase ROS levels can overwhelm the antioxidant capacity of cancer cells, leading to oxidative stress-induced cell death (Trachootham et al., 2009).

2.7 Tumor Necrosis Factor-Alpha (TNF-α) in Cancer

TNF-α is a pro-inflammatory cytokine that plays complex roles in cancer biology, including tumor promotion and suppression. Initially identified for its ability to induce hemorrhagic necrosis in tumors, TNF-α is now known to have dual roles, depending on the context and tumor microenvironment (Aggarwal, 2003).

2.8 TNF-α Signaling Pathways

TNF-α exerts its effects through binding to two receptors: TNF receptor 1 (TNFR1) and TNF receptor 2 (TNFR2). TNFR1 is ubiquitously expressed and mediates most of the biological effects of TNF-α, including the activation of NF-κB, MAPK, and apoptosis signaling pathways. TNFR2 is mainly expressed in immune cells and endothelial cells and primarily activates NF-κB and promotes cell survival and proliferation (Wajant et al., 2003).

2.9 TNF-α-Induced Apoptosis and Necroptosis

TNF-α can induce apoptotic cell death through the extrinsic pathway, involving the formation of the death-inducing signaling complex (DISC) and the activation of caspase-8. In conditions where caspase-8 is inhibited, TNF-α can trigger necroptosis,

a programmed form of necrotic cell death mediated by receptor-interacting protein kinase 1 (RIPK1) and RIPK3 (Wang et al., 2008).

2.10 TNF-α in Tumor Promotion

In addition to its role in inducing cell death, TNF-α can promote tumor growth and metastasis by activating NF-κB and MAPK signaling pathways, which enhance cell proliferation, survival, angiogenesis, and inflammation. The pro-tumorigenic effects of TNF-α are particularly evident in the tumor microenvironment, where it can modulate the behavior of tumor cells and stromal cells (Balkwill, 2009).

2.11 Therapeutic Targeting of TNF-α

Given its dual roles in cancer, therapeutic strategies targeting TNF-α signaling must be carefully designed to achieve anti-tumor effects while minimizing pro-tumorigenic activities. Approaches include the use of TNF-α inhibitors, such as monoclonal antibodies and soluble TNF receptors, as well as agents that selectively induce TNF-α-mediated cell death pathways (Van Horssen et al., 2006).

2.12 Combination Therapies in Glioma Treatment

The complex biology of gliomas necessitates the use of combination therapies that target multiple pathways simultaneously. Combining ROS-inducing agents with pro-inflammatory cytokines like TNF-α represents a promising strategy to enhance glioma cell death.

2.13 Synergistic Effects of ROS and TNF-α

Combining ROS-inducing agents with TNF-α can result in synergistic cell death, as ROS can potentiate TNF-α-induced apoptosis and necroptosis. ROS can increase mitochondrial membrane permeability, leading to the release of cytochrome c and the activation of the intrinsic apoptotic pathway. Additionally, ROS can modulate the

activity of NF-κB and MAPK signaling pathways, influencing the cellular response to TNF-α (Fulda, 2009).

2.14 Preclinical Studies

Preclinical studies have demonstrated the potential of combining ROS-inducing agents with TNF-α to enhance anti-tumor effects. For example, combining the ROS-inducing agent arsenic trioxide with TNF-α has been shown to synergistically induce apoptosis in glioma cells (Kanzawa et al., 2003). Similarly, the combination of TNF-α with the ROS-inducing agent menadione has been shown to enhance cell death in glioma cells (Yamanaka et al., 2001).

2.15 Clinical Implications

While preclinical studies provide promising evidence for the efficacy of combination therapies, clinical translation requires careful consideration of dosing regimens, toxicity, and patient selection. Clinical trials are needed to evaluate the safety and efficacy of combining ROS-inducing agents with TNF-α or other pro-inflammatory cytokines in glioma patients.

2.16 Interleukin-6 (IL-6) and Glioblastoma

IL-6 is a pro-inflammatory cytokine that plays a crucial role in glioblastoma progression. It promotes tumor growth, survival, and angiogenesis through the activation of the JAK/STAT3 signaling pathway. Elevated levels of IL-6 in the tumor microenvironment are associated with poor prognosis and resistance to therapy Sansone et al., 2007). IL-6 can also influence the expression of miRNAs in glioblastoma cells, contributing to the regulation of tumor-promoting pathways.

2.17 Interleukin-10 (IL-10) and Glioblastoma

IL-10 is an anti-inflammatory cytokine with immunosuppressive properties. In the context of glioblastoma, IL-10 can promote tumor immune evasion by inhibiting

the activation and function of immune cells, such as T cells and macrophages (Couper et al., 2008). The interplay between IL-10 and miRNAs in glioblastoma cells can further modulate the immune response and tumor progression.

Chapter 3

Methodology

3.1 Research Design

The research design in the flowchart appears to focus on investigating the impact of hydrogen peroxide (H_2O_2) and tumor necrosis factor-alpha (TNF-α) on the viability of different human glioma cell lines, including YKG1, LN18, Huvec, and U87. Here's a detailed breakdown and explanation of the steps outlined in the design:

3.1.1 Treatment of cell lines.

- Cells Used: YKG1, LN18, Huvec, and U87 (glioma cell lines)
- The cells are treated with two different conditions:
- TNF-α (Tumor Necrosis Factor-α)
- H_2O_2 (Hydrogen Peroxide)

The goal is to assess how varying concentrations of these compounds impact the viability and behaviour of these cancer cell lines.

3.1.2 Optimization and assays.

- MTT Assay: The MTT assay is used to determine cell viability. It helps identify the optimal concentration of TNF-α and H_2O_2 for subsequent experiments. Multiple concentrations (likely 6 for both TNF-α and H_2O_2) are tested to find the most effective one.
- ROS Assay: This is used to measure reactive oxygen species (ROS) levels in the cells. Since H_2O_2 is a known inducer of oxidative stress, the ROS assay will help quantify oxidative damage.

3.1.3 Grouping experimental conditions. Four experimental groups are created to explore different treatment combinations using the optimal concentrations of TNF-α and H_2O_2, allowing for a more comprehensive analysis.

3.1.4 Measuring cell viability and migration.

- MTT Assay: Cell viability is measured in all treatment groups, confirming the cytotoxic or protective effects of the treatments.
- Wound Healing Assay: This is used to measure the cell migration capacity. The ability of cells to migrate is an important indicator of cancer cell aggressiveness and metastasis potential.

3.1.5 Analysing inflammatory factor expression.

- Gene Expression Analysis: Pro-inflammatory and anti-inflammatory factors are assessed by analysing the expression levels of key cytokines like IL-6 and IL-10.
- RNA Isolation, cDNA Synthesis, and qPCR: These methods are used to measure cytokine expression, allowing for insights into how the treatments impact inflammatory responses within the cells.

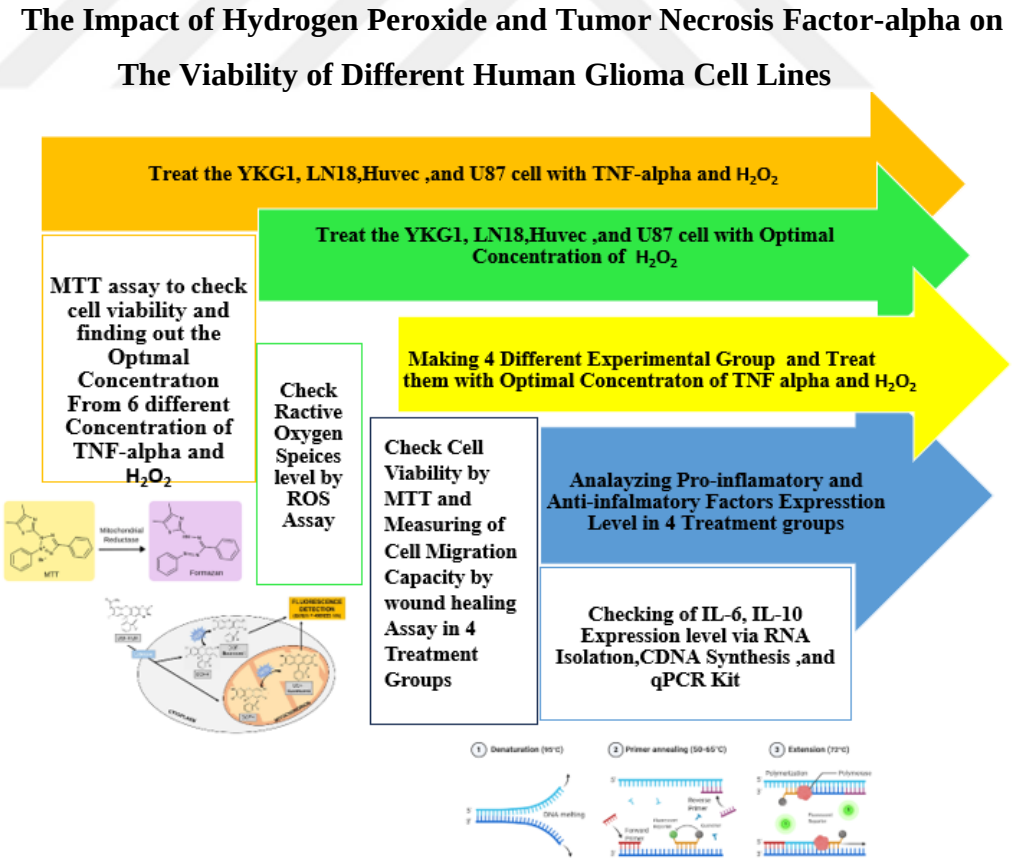

Figure 1. Flowchart of the research design for study (BioRender, n.d.).

3.2 Data Collection

3.2.1 Data collection instrument and materials. For this research, a range of items were necessary, encompassing specific chemicals and enzymes, dedicated kits, machinery and tools, single-use plastic items, and forward primers specific to miRNA.

Table1

List of Chemicals and Enzymes

Chemical	Brand Name & Catalog Number
Absolute Ethanol	ISOLAB/Germany Catalog #920.026.2500
10X Phosphate Buffered Saline PBS	THERMOFISHER Gibco Catalog #10010015
DMEM- Dulbecco's Modified Eagle Medium	THERMOFISHER Gibco Catalog #41966029
Trypsin	THERMOFISHER Gibco Catalog #25200056
Penicilin/Streptomycin	THERMOFISHER Gibco Catalogy #15140122
Fetal Bovine Serum (FBS)	GIBCO/UK Catalog# 10270-106
Exosome-Depleted Fetal Bovine Serum Qualified One Shot ™	Gibco/USA Reference# A27208-03
Nuclease-Free Water / PCR Grade Water	LETGEN Reference# 7E60212C
Hydrogen Peroxide (H_2O_2) 30%	VWR BDH PROLABO CHEMICALS Catalog #BDH7690-3
Trypan Blue Solution	AMRESCO Catalog #1184C222

Table 2

List of Kits

Kit	Brand Name & Catalog Number
cDNA Synthesis Kit (5X)	NUCLEOGENE Catalog# NGMM019
qPCR SYBR Green Master Mix Kit (2x)	NUCLEOGENE Catalog# NGMM007
Thiazolyl blue tetrazolium bromide (MTT)	Sigma-Alderich/USA Catalog# CT02

Table 3

List of Equipments

Equipment	Brand Name
Leica DMIL Inverted Microscope	Leica, Germany
Centrifuge	Thermo Fisher, USA
Microcentrifuge 16	Beckman Coulter, USA
Cell Culture Incubator	Panasonic, USA
Vortex	Scilogex, UK
Electronic Balance	Shimadzu, Japan
Ultra-Low Temperature Freezer (-80°c)	DAIHAN Scientific, Korea
Refrigerator (+4°c and -20°c)	PROFiLO/Turkey
Cell Cytometer	HIRSCHMANN/Germany
Laminar Flow Hood (Telstar Bio II advance)	Telstar®/USA
Hidex Sense Microplate Reader	Hidex/Finland
T100 Thermal Cycler PCR	Bio-Rad, USA
CFX96 Touch Deep Well Real Time PCR System	Bio-Rad, USA
UV/Vis Nano Spectrophotometer	Nabi
Water Bath	WiseBath®/Germany

Table 4

List of Disposable Plasticware

Plasticware	Brand Name
T25, T75 Cell Culture Flasks	NEST
96-well plates	NEST
6-well plates	NEST
Serological pipettes	NEST
Micro-pipette (0.2-2 µl)	NEST
Micro-pipette (0.2-10 µl)	NEST
Micro-pipette (2-20 µl)	NEST
Micro-pipette (20-200µl)	NEST
Micro-pipette (10-100µl)	NEST
Micro-pipette (100-1000µl)	NEST
Micro-pipette tips	NEST
15ml Falcon Tubes	NEST
50ml Falcon Tubes	NEST
Gloves	NEST

3.3 Data Collection Procedures

3.3.1. U87, LN18, YKG1, and HUVEC cell line characteristics and differentiation.

3.3.1.1 Origin and characteristics of U87 cell line. U87 is a human glioblastoma cell line derived from a malignant glioma tumor. These cells are known for their rapid proliferation and aggressive behaviour. They are often used in glioblastoma research due to their high tumorigenicity and ability to form tumors in immunocompromised mice (Ponten & Macintyre, 1968). U87 cells exhibit mutations in the TP53 gene and amplification of the EGFR gene, which are common alterations in glioblastomas. These genetic features make U87 a representative model for studying the molecular mechanisms underlying glioblastoma pathogenesis (Westphal et al., 1999). U87 cells are widely used in glioblastoma research because they provide a robust model for

studying tumor biology, drug responses, and the effects of genetic and epigenetic modifications. Their aggressive nature and high tumorigenicity make them suitable for in vivo studies and preclinical testing of therapeutic agents.

3.3.1.2 Origin and characteristics of LN18 cell line. LN18 is another human glioblastoma cell line. These cells are known for their moderate growth rate and invasive properties. Unlike U87, LN18 cells exhibit a more differentiated phenotype, which can influence their behavior and response to treatments (Weller et al., 1998). LN18 cells have mutations in the PTEN gene and exhibit wild-type TP53, distinguishing them from U87 cells. This genetic profile provides a different perspective on glioblastoma biology and treatment responses (Ishii et al., 1999). LN18 cells are used in glioblastoma research to provide a comparative model to U87 cells. Their distinct genetic and phenotypic characteristics allow researchers to explore the heterogeneity of glioblastomas and evaluate the efficacy of therapeutic agents across different genetic backgrounds.

3.3.1.3 Origin and characteristics of YKG1 cell line. YKG1 is a glioblastoma cell line derived from a human glioblastoma multiforme tumor. These cells are known for their invasive behavior and ability to form spheroids, which are indicative of tumorigenic potential and cellular heterogeneity (Nakada et al., 2010). YKG1 cells exhibit mutations in key oncogenes and tumor suppressor genes, including EGFR and PTEN. These genetic alterations contribute to their aggressive phenotype and resistance to conventional therapies (Nakada et al., 2010). YKG1 cells are used in glioblastoma research to study tumor invasion, spheroid formation, and the effects of targeted therapies. Their invasive properties and ability to form spheroids make them suitable for investigating the mechanisms of tumor progression and metastasis.

3.3.1.4 Origin and characteristics of HUVEC cell line. Human Umbilical Vein Endothelial Cells (HUVEC) are derived from the endothelium of veins from the human umbilical cord. These cells are commonly used as a model for studying endothelial cell biology, angiogenesis, and vascular functions (Jaffe et al., 1973). HUVECs exhibit characteristics typical of endothelial cells, including the expression of markers such as CD31, VE-cadherin, and von Willebrand factor. They can form capillary-like

structures in vitro, making them a valuable model for studying angiogenesis (Jaffe et al., 1973). HUVECs are used in glioblastoma research to study the interactions between tumor cells and the vascular system. Angiogenesis is a critical process in tumor growth and metastasis, and HUVECs provide a relevant model for investigating the effects of therapeutic agents on endothelial cell function and the tumor microenvironment.

3.3.2 Cell culture conditions.

3.3.2.1 Media utilization. The cells are cultured in a high glucose variant of DMEM, which is supplemented with 10% FBS. While not a mandatory inclusion, Pen/Strep at a 1X concentration is tolerated by the cells.

- DMEM: Sourced from Sigma D5796, this formulation includes 4500 mg/L glucose, L-glutamine (0.584 g/L), and sodium bicarbonate (3.7 g/L), but lacks sodium pyruvate.
- Fetal Bovine Serum (US): Provided by ATCC under the catalog number 30-2020.
- Penicillin/Streptomycin, Liquid: Manufactured by Biochrome AG, A2213, this product comprises 10,000 units of penicillin and 10,000 µg of streptomycin per milliliter.

3.3.2.2 Culture methodology. The cells adhere and proliferate on standard tissue culture plastics without the need for any special coatings. During the first few days after thawing, cell density is not a critical factor as this time is mainly for cell recovery. Once the cells show healthy growth, they should be seeded at a density appropriate for the intended experiment. Typically, the culture medium is replaced every 2 to 3 days, depending on the cell growth rate. When cultures reach around 80% confluency, they should be split at a ratio between 1:10. Cells are detached from plates or flasks using a 0.25% trypsin-EDTA solution (about 500 microliters for a 60-100 mm plate or a T25 flask) for 5 minutes at 37°C, followed by a 10-fold dilution with DMEM (CELLutions Biosystems Inc., Cerdalane - Ontario, 2016).

The glioma cell line, generously provided by Dario Bonanomi from the San Raffaele Scientific Institute in Milan, Italy, was cultured in Dulbecco's Modified Eagle

Medium (DMEM) supplemented with 2 mM glutamine (Corning, New York, US), 10% fetal bovine serum (FBS), 100 U/mL penicillin, and 100 µg/mL streptomycin (Corning). Cells were maintained at 37°C in an incubator with 95% humidity and 5% CO2. For processing, 10^4 cells were harvested and centrifuged for 5 minutes at 1500 rpm, then the cell pellet was resuspended in 10 ml of DMEM (Stanzione et al., 2021).

3.3.3 Preparation of H_2O_2 and TNF-alpha. Hydrogen Peroxide (H_2O_2): With a mass of 0.1 mg and a molecular weight of 32987 Da, the desired concentration for the GLP-1 ligand is 10 micromolar, resulting in a stock solution volume of 3.0315 mL.

Tumor Necrosis Factor-alpha (TNF-alpha): With a mass of 0.1 mg and a molecular weight of 4186.66 Da, to achieve the desired concentration of 10,15,20,25,30, and 50 micromolar, 2.38885 mL of the stock solution is required.

For this experiment, the required concentrations of H_2O_2 and TNF-alpha will be 10, 100, 300,400,500 and 600 micromolar for each 1×10^4 cells per well.

3.4 Procedures

3.4.1 The effect of H_2O_2 and TNF alpha on cell viability: MTT.

1. MTT solution is added (20 microliters).
2. Incubation is carried out at room temperature for a duration ranging from 30 minutes to 3 hours.
3. Solvent solution is added (150 microliters).
4. An incubation period of 15 minutes at room temperature is observed.
5. The plate is read at a wavelength of 570 nm (Meerloo, Kaspers, & Cloos, 2011).

MTT total volume would be number of wells multiply 30 microliters of MTT.

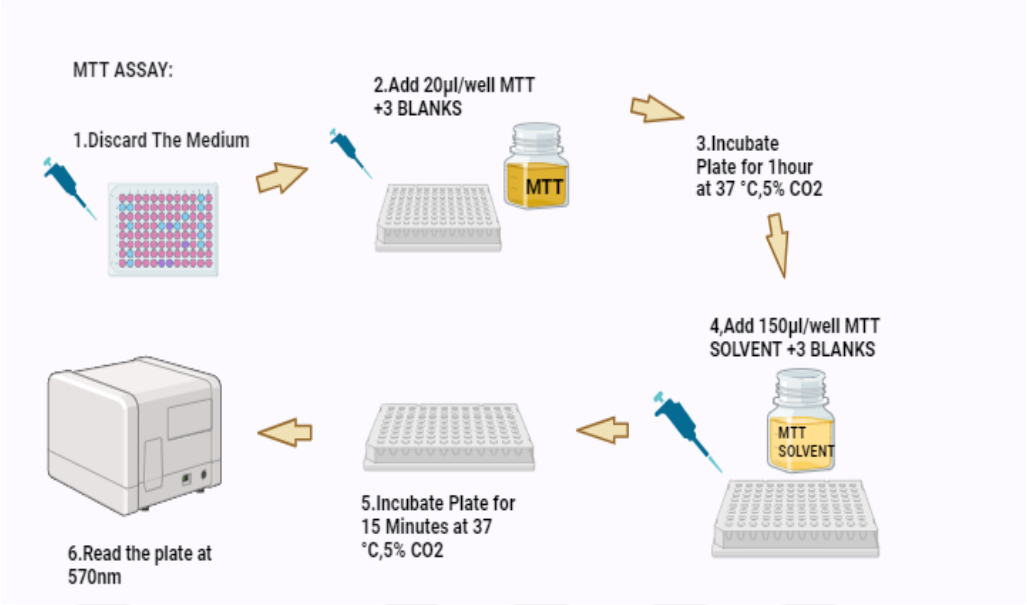

Figure 2. MTT assay steps (BioRender, n.d.).

3.4.2 The effect of H_2O_2 and TNF alpha on reactive oxidative stress level: ROS.

1.Medium would be removed from each well.

2. 80 microliters of 50 micromolar DCFDA should be added per well.

3.Cells would be incubated 30 minutes to 2 hours.

4.All medium would be removed from each well.

5.Cells would be washed with PBS once.

6.150 microliter RPMI would be added to each well.

7.Plate would be read at 490 to 540 nm wavelength by plate reader.

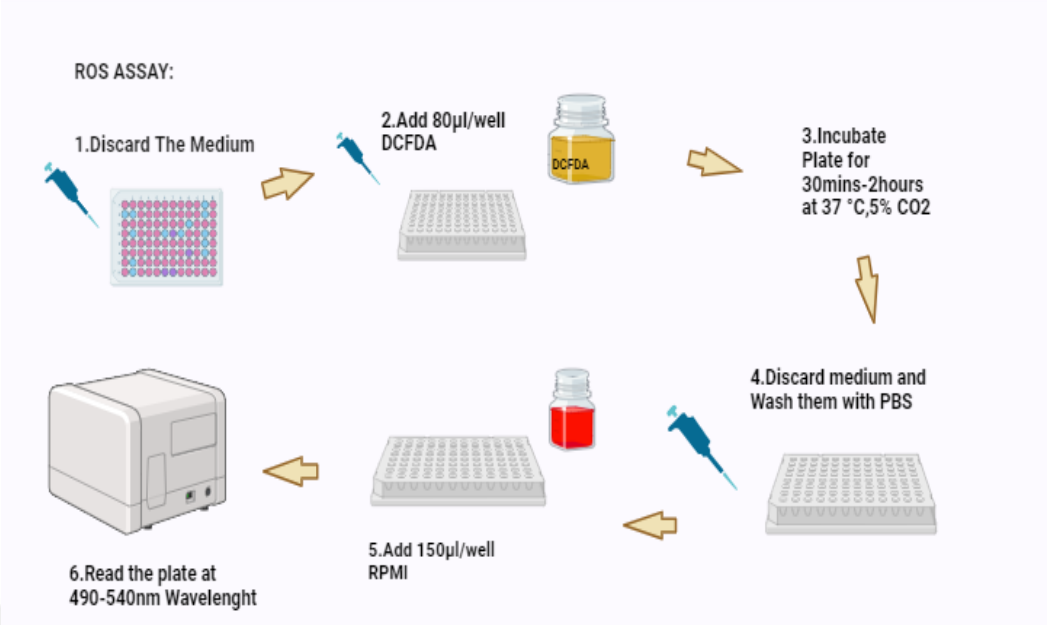

Figure 3. ROS assay steps (BioRender, n.d.).

3.4.3 Scratch assay protocol.

Procedure:

1. Cell Seeding:
    - glioma cells were seeded into a 6-well plate at $2x10^5$ cells per well to achieve 90% confluency in 24-48 hours (Stanzione et al., 2021).
    - They were Incubated at 37°C with 5% CO2.
2. Creating the Scratch:
    - Once confluent, were used a sterile 10 µL pipette tip to make a straight scratch across each well. Applied consistent pressure to maintain uniform scratch width (CELLutions Biosystems Inc., Cerdalane - Ontario, 2016).
3. Adding Treatment:
    - Treatments were added (e.g., H_2O_2, TNF-alpha) at desired concentrations.

4. Incubation:
    - Cells were Incubated at 37°C with 5% CO2 for 24-48 hours, ensuring consistent incubation conditions.
5. Imaging:
    - Images were captured of the scratch area immediately after scratching (0 hours) and at intervals (e.g.24, and 48 hours) using a microscope with a camera.
    - The same area was imaged each time for consistency (Stanzione et al., 2021).
6. Data Analysis:
    - Image analysis software was used (e.g., ImageJ) to measure the scratch area and cell migration.
    - Calculate wound closure percentage using the formula: Wound Closure (%) = (Initial Scratch Area−Final Scratch Area/Initial Scratch Area) ×100

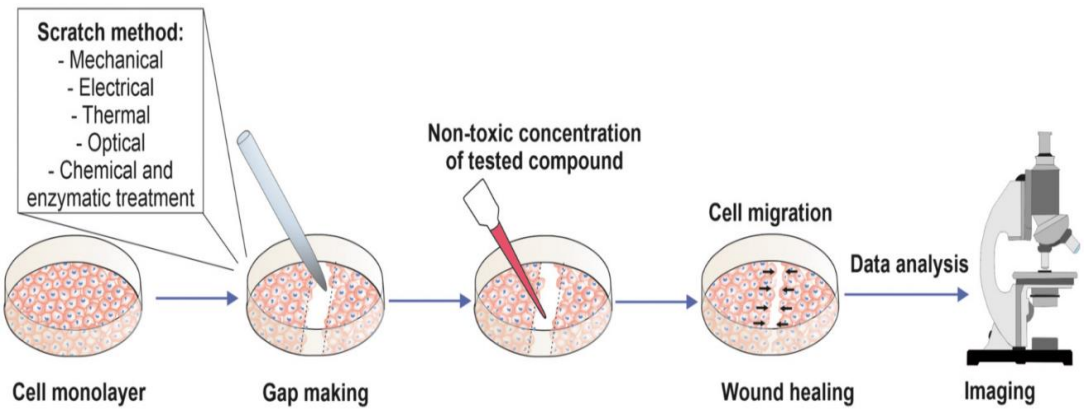

Figure 4. Scratch assay steps (Gurgul, Janczy-cempa, Gajda-morszewski, & Mazuryk, 2022).

3.4.4 RNA extraction process.

1. Medium would be removed.
2. Cells would be rinsed by using PBS.
3. Following the removal of PBS, introduce between 0.10 and 0.25 percent of Trypsin would be added and incubated for 5 minutes 37°C with 5% CO,
4. After cell detachment is observed, incorporate the medium and shift the contents into a 2ml tube for centrifugation at 300g for 5 minutes.
5. Supernatant must be discarded.
6. 450 microliter per tube lysis buffer must be added and incubate for 10 minutes.
7. Centrifuge the solution for two minutes at a force of 14000G to prevent column blockage by solid fragments.
8. Gently extract the clear liquid layer above and place it into a freshly prepared microcentrifuge tube, sizing between 1.5 and 2 ml.
9. 450 µl per tube ethanol must be added and vortex for 1 min/tube.
10. The resultant solution would be relocated into a spin column housed within a collection tube, then execute a centrifugation at 11000xg for a span of 30 seconds. Following this, the collection tube's contents should be removed, with the spin column being reinserted into it.
11. 400 µl of the primary wash buffer would be added into the spin column, followed by centrifugation at the same speed for another 30 seconds.
12. Afterward, the spin column would be cleared and replaced into the emptied collection tube.
13. 700 µl of the secondary wash buffer would be added into the spin column and subject it to centrifugation at 14000xg for one minute. Subsequently, the used collection tube would be removed and, the spin column must be transferred into a sterile, nuclease-free microcentrifuge tube, sized between 1.5 and 2 ml.
14. 100 µl of elution buffer would be deposit at the spin column's center for RNA elution and, followed by centrifugation at 11000xg for two minutes (Specifications et al., n.d.)

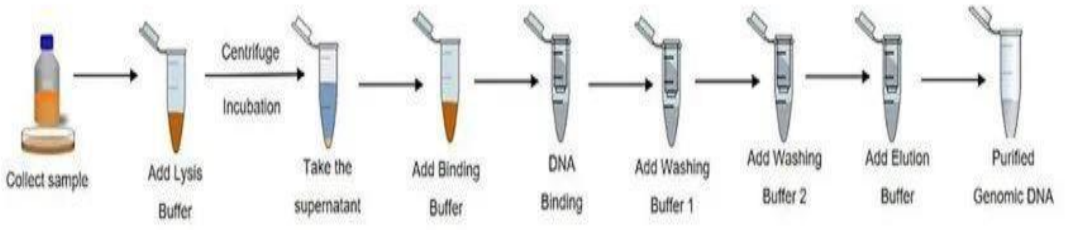

Figure 5. RNA isolation (Nucleogene, n.d.).

Table 5

NucleoGene QuickEx RNA Extraction Kit

Supplied Material	50Test	100Test	250Test
Lysis Buffer	40ml	80ml	20m
Wash Buffers I	20ml	40ml	100ml
Wash Buffers II	7ml	14ml	35ml
DNase I	1 vial	1 vial	1 vial
DNase I Buffer	2.25ml	4.5ml	11.25ml
Elution Buffer	5ml	10ml	25ml
Spin Column	50	100	250
Collection Tubes	50	100	250
User Guide	1	1	1

3.4.5 cDNA synthesis.

1. The necessary chemicals would be Mixed in either 0.2ml micro-tubes or within the confines of a 96-well plate, ensuring they are kept cool on ice.
2. After initiating each reaction, it's important to lightly vortex to ensure the mixture is even. Then, a quick spin is needed to gather all elements at the base of the tube. Following this, the blend should undergo a warming period for 5

minutes at 25°C, continue for 30 minutes at 50°C, spend another 5 minutes at 85°C, before finally being maintained at 4°C.

3. Once the synthesis of cDNA is finalized, a fraction, ranging from one-fifth to one-tenth (2-4µl), of the end product should be allocated for PCR enhancement. Should there be a need, the synthesized cDNA can be thinned out using 10mM Tris-HCl (with a pH of 8.0) and 0.1mM EDTA, then preserved at -20°C.

Table 6

cDNA Synthesis Component

cDNA Synthesis Component	*Volume for 20ul*	*Final Concentration*
NucleoGene cDNA synthesis kit(5x)	*4µl*	*1x*
RNA template	*variable*	*1µg to 10pg total RNA*
RNase/DNase-free water	*variable*	
Total Volume(ul)	*20µl*	

3.4.6 Real-time polymerase chain reaction (qPCR). Primer Configuration Tailored primers targeting IL-6 and IL-10 genes, alongside a reference gene (as GAPDH) for internal normalization, will be crafted or procured. This step ensures the primers exclusively amplify the intended gene sequences, thereby eliminating unintended amplification.

Table7

Primer Design

IL-6	Forward primer CCCACCGGGAACGAAAGAGA
	Reverse primer TCTCCTGGGGGTATTGTGGAG
	Sequence (5'->3') Product length 81
IL-10	Forward primer AGGGCACCCAGTCTGAGAAC
	Reverse primer TTGGCAACCCAGGTAACCCTTA
	Sequence (5'->3') Product length 179

Following the qPCR kit provider's guidelines, a reaction mixture will be concocted. This concoction will encompass DNA polymerase, nucleotides (dNTPs), tailored primers for both IL-6 and IL-10 plus a control, either a fluorescent marker like SYBR Green or a specific probe, and the converted DNA (cDNA) sample. This mixture will then be allocated into qPCR plate wells, complemented by a measured quantity of cDNA.

The qPCR device will be configured to execute specified thermal cycling parameters, typically initiating with a phase of initial denaturation, succeeded by 35-40 cycles of sequential denaturation, annealing, and elongation phases. The precise temperature settings and timing will be adjusted according to the selected primers and the specific qPCR kit.

Through analysis of the amplification graphs, the cycle threshold (Ct) values corresponding to IL-6, IL-10 and the reference gene in each specimen will be ascertained. A relative quantification technique, such as the ΔΔCt method, will then be employed to deduce the expression levels of IL-6 and IL-10, normalizing these against the reference gene to mitigate variance in cDNA volume and reaction efficacy.

Confirming the Results:

To affirm the accuracy and consistency of the qPCR findings, it's recommended to replicate the tests, ideally with biological triplicates, thereby reinforcing the data's dependability and reproducibility.

Table 8

Reaction Assembly

Component	Volume for 20µL
NucleoGene qPCR Sybr Green Master Mix (2x)	10µl
Forward primer	variable
Reverse primer	variable
Nuclease-free water	variable
template	2-5µl
Final Volume(µl)	20µl

Table 9

Real Time PCR Protocol

	Standard Cycling	3-Step Cycling
Initial denaturation	95c, 15min	95c, 15 min
Denaturation	95c, 10 to 15s	95c ,10 to15s
Annealing	60c, 30 to 60s	55 to 65c ,30 to 60s
Extension/elongation		68 to 72c ,10s
PCR cycling (30-45 cycles)		

3.5 Study Limitations

3.5.1 Specificity of cell lines. This research employs selected glioma cell lines (YKG1, LN18, U87) and human endothelial cells (HUVEC) to explore the effects of treatments. Although these lines offer valuable insights into glioma characteristics, they do not fully capture the range of glioma variations encountered in patients. Different glioma subtypes and cells sourced directly from patients might respond differently to hydrogen peroxide (H_2O_2) and TNF-α, which could restrict the broader applicability of the results.

3.5.2 In vitro experimental environment. The use of in vitro cell culture models allows for a controlled investigation of cellular responses. However, these simplified models do not reflect the complexity of the tumor microenvironment found within the human body, which includes interactions with various cell types, extracellular matrices, and blood vessels. As a result, findings from these experiments may not be fully indicative of what occurs in a living organism.

3.5.3 Concentration range constraints. The study focuses on specific concentrations of H_2O_2 and TNF-α to examine their impact on cell survival and behavior. While a range of concentrations is tested to identify optimal doses, this approach might overlook subtler, dose-dependent effects or the influence of lower concentrations that are more relevant to physiological conditions.

3.5.4 Measurement of oxidative stress. The reactive oxygen species (ROS) assay used here provides a single-point measure of oxidative stress within the cells. However, oxidative stress is a dynamic process that changes over time, and this assay might not fully capture the temporal variations or the long-term consequences of oxidative stress on cell function and viability.

3.5.5 Limitations of the scratch assay. The scratch (wound healing) assay is a common method for assessing cell migration. However, this technique has certain limitations, including inconsistencies in scratch size and the pressure applied during the scratch. Additionally, it does not replicate the three-dimensional invasion and migration processes that occur within actual tumors, limiting its relevance to the in vivo behavior of glioma cells.

3.5.6 Assessment of inflammatory markers. While the study utilizes qPCR to measure the expression of cytokines like IL-6 and IL-10, it only reflects the mRNA levels of these markers. This method does not provide direct information about the protein expression or activity, which is crucial for understanding their functional impact on glioma cell behavior and tumor progression.

3.5.7 Variability in cell culture. Small variations in culture conditions, such as temperature, media composition, and the number of cell passages, could influence the outcomes of the experiments. Despite efforts to standardize these conditions, minor inconsistencies might introduce variability into the results, potentially affecting the study's reproducibility.

3.5.8 Absence of in vivo validation. Since the study is solely conducted using in vitro methods, there is no validation in animal models or clinical samples. Therefore, the effects observed here on glioma cell behavior cannot be directly correlated with patient outcomes or clinical settings, limiting the study's translational potential.

These limitations highlight the necessity for further research, including studies involving more diverse glioma models and in vivo experiments, to gain a more comprehensive understanding of how H_2O_2 and TNF-α affect glioma development and potential treatment responses.

Chapter 4

Findings

4.1 MTT Cell Viability Analysis of the Optimal H_2O_2 Concentration

H_2O_2 was used to induce oxidative stress in HUVEC, LN18, YKG1, and U87 cell lines. Six different concentrations of hydrogen peroxide (100, 200, 300, 400, 500, and 600 µM) were applied, and after 24 hours, the MTT test was performed to identify the optimal concentration that caused a significant decrease in cell viability across all four cell lines.

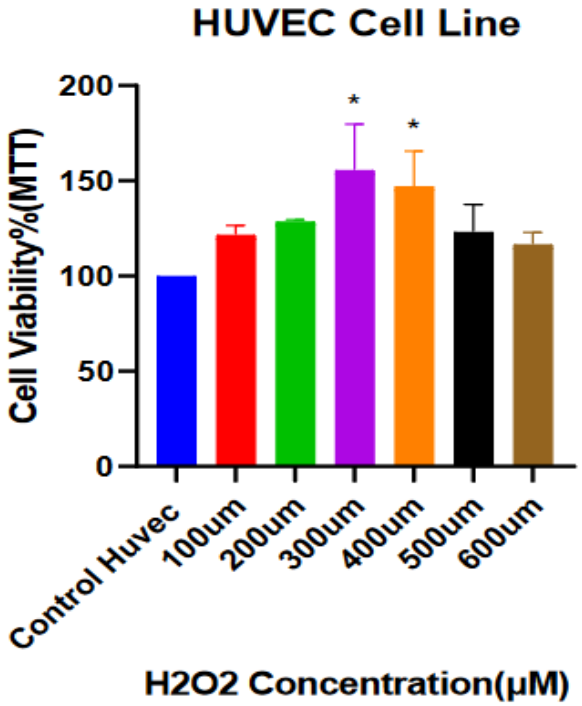

Figure 6. Cell viability percentages of HUVEC with different H_2O_2 concentrations. Analysis was performed by one-way ANOVA, **** $p < 0.0001$, *** $p < 0.001$, ** $p < 0.01$, * $p < 0.05$.

The graph demonstrates that HUVEC cell viability is generally unaffected at lower hydrogen peroxide (H_2O_2) concentrations (100-200 µM). However, there is a significant increase in viability at 300-400 µM, peaking around 150-160% at 400 µM. Beyond this, cell viability begins to decrease at higher concentrations (500-600 µM),

though it remains above 100%. This suggests an optimal H_2O_2 concentration range (300-400 µM) for stimulating HUVEC cell proliferation, with higher concentrations becoming increasingly toxic. Cell viability remains relatively consistent, staying close to control levels. These concentrations are suitable for exploring homeostatic responses or mild stress conditions without inducing significant cytotoxicity.

Notable increases in cell viability are observed at 400 µM and 500 µM, indicating potential proliferative or adaptive effects at these levels. These concentrations could be ideal for studying protective cellular responses or investigating mechanisms of stress resilience.

A noticeable drop in cell viability occurs at 600 µM, suggesting the onset of cytotoxic effects. This concentration could be useful for examining oxidative damage or triggering apoptosis pathways.

Future experiments should aim to verify the mechanisms behind the increased viability at 400 µM and 500 µM. Testing for oxidative stress markers or other indicators of adaptive responses may provide insights into how HUVEC cells manage oxidative stress. Utilizing additional assays like flow cytometry or live/dead staining can confirm these observations and offer more clarity on cell death or survival mechanisms.

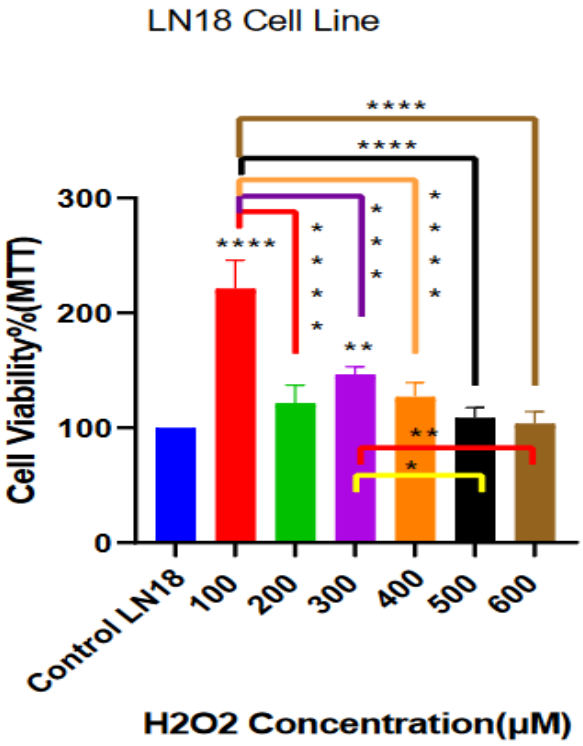

Figure 7. Cell viability percentages of LN18 with different H_2O_2 concentrations. Analysis was performed by one-way ANOVA, **** $p < 0.0001$, *** $p < 0.001$, ** $p < 0.01$, * $p < 0.05$.

As shown in the chart, LN18 cells exhibited varying levels of viability when exposed to different concentrations of hydrogen peroxide (H_2O_2) using the MTT assay. A concentration of 100 µM H_2O_2 significantly increased the proliferation potential of LN18 cells to about 200% of the control level ($p < 0.0001$), indicating enhanced cell viability. However, concentrations of 200-300 µM H_2O_2 resulted in a decrease in cell viability to around 150-175% compared to the control, though these levels remained above the control, suggesting initial signs of oxidative stress ($p < 0.01$). Concentrations of 400-600 µM H_2O_2 led to a marked decrease in cell viability, with percentages dropping closer to 100%, indicating significant oxidative stress and cell death at these concentrations ($p < 0.0001$).

Concentrations in the range of 100 µM to 200 µM show an increase in cell viability, making them suitable for studies focusing on cell proliferation or stress adaptation. Further research is recommended to understand the mechanisms behind this increase, such as potential antioxidant effects.

For research on cell death and oxidative damage, higher concentrations starting from 400 µM should be the focus, as they demonstrate a clear reduction in cell viability. The most substantial cell death occurs at 500 µM and 600 µM, ideal for studies on apoptosis or necrosis pathways.

Additional experiments should explore oxidative stress markers and cell death pathways triggered by H_2O_2 in the 300 µM to 600 µM range. Other assays like live/dead staining or flow cytometry can further confirm MTT results, and low-dose H_2O_2 studies could reveal mechanisms related to therapeutic resistance.

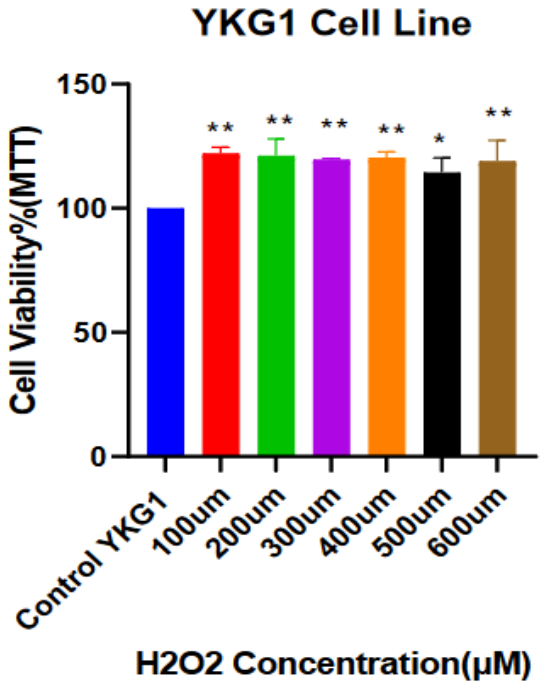

Figure 8. Cell viability percentages of YKG1 with different H_2O_2 concentrations. Analysis was done by one-way ANOVA, **** $p < 0.0001$, *** $p < 0.001$, ** $p < 0.01$, * $p < 0.05$.

The YKG1 cell line shows increased viability at lower H_2O_2 concentrations (100-300 µM), peaking around 125-130%. Viability slightly decreases at 400-500 µM but remains above 100%. Interestingly, at 600 µM, viability increases again to about 115-120%, indicating a possible adaptive response. Overall, the data suggests that YKG1 cells generally respond positively to H_2O_2, with varying effects depending on the concentration.

The graph demonstrates that as the concentration of H_2O_2 increases, the YKG1 cell line viability generally increases, peaking at 300–600 µM concentrations. Therefore, further investigation into this surprising increase in cell viability at higher H_2O_2 concentrations is recommended. Since H_2O_2 is expected to reduce cell viability due to its oxidative nature, the increase in viability suggests a need to reevaluate its role as a standalone treatment for this particular cell line. Exploring different concentrations or exposure times might be necessary to induce the expected cytotoxic effect.

The data indicates that YKG1 cells might activate protective mechanisms in response to oxidative stress at these H_2O_2 levels. Further studies could explore underlying pathways that allow the cells to survive and even thrive at these concentrations. Based on this unexpected increase in cell viability, future research should consider combining H_2O_2 with other agents, such as TNF-α, to assess if combination treatments might overcome the resistance or protective responses observed at higher H_2O_2 levels.

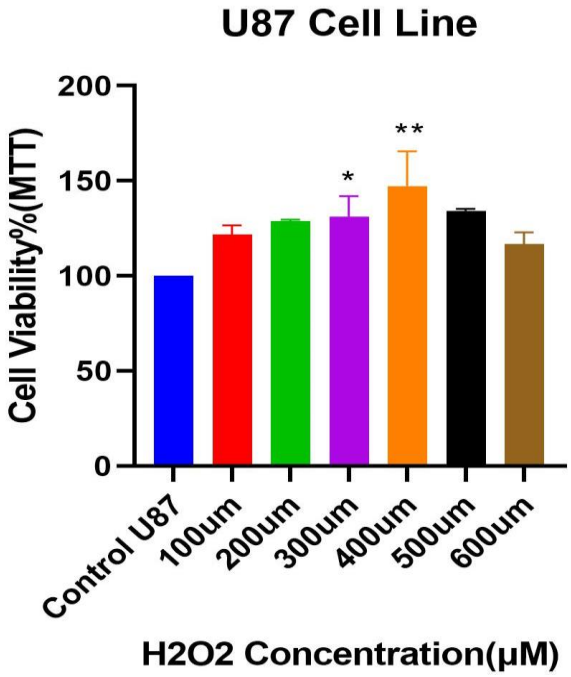

Figure 9. Cell viability percentages of U87 with different H_2O_2 concentrations. Analysis was performed by one-way ANOVA, **** $p < 0.0001$, *** $p < 0.001$, ** $p < 0.01$, * $p < 0.05$.

From 100 µM to 500 µM, U87 cells demonstrate increasing viability, with a peak at 500 µM, suggesting the cells may benefit from moderate oxidative stress, potentially activating survival or protective mechanisms. At 600 µM, cell viability declines, indicating that this concentration starts to exert a negative effect on the cells, possibly due to excessive oxidative damage that surpasses the cells' ability to counteract the stress. U87 cells appear to exhibit a hormetic response to H_2O_2, where lower to moderate concentrations increase cell viability, but higher concentrations lead to reduced viability.

This pattern of response could imply that U87 cells have a robust oxidative stress response system that allows them to survive under conditions that would typically be harmful to other cell types. Further research into the underlying molecular mechanisms could help explain this increased viability under oxidative conditions.

4.2 MTT Cell Viability Analysis of the Optimal TNF-alpha Concentration

Inflammation was induced in HUVEC, LN18, YKG1, and U87 cell lines using TNF-alpha. Hydrogen peroxide was applied at six different concentrations (10, 15, 20, 25, 30, and 50 ng/ml), and after 24 hours, an MTT assay was conducted to determine the most effective concentration that significantly reduced cell viability in all four cell lines.

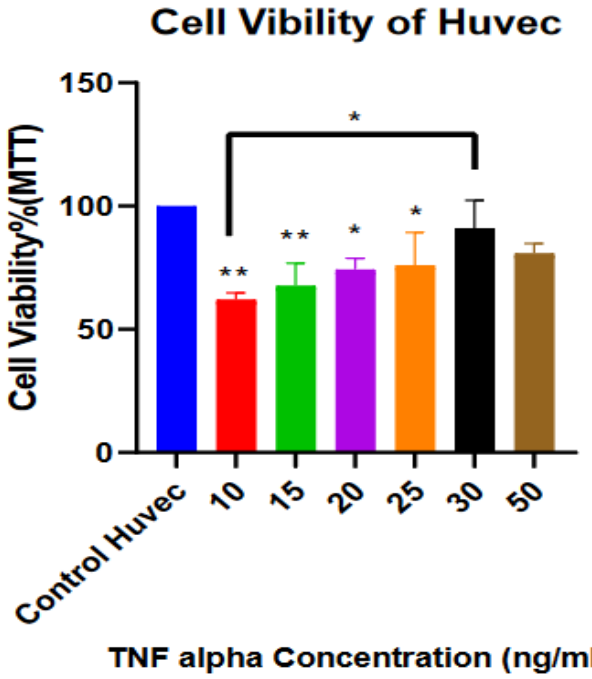

Figure 10. Cell viability percentages of HUVEC with different TNF alpha concentrations. Analysis was done by one-way ANOVA, **** $p < 0.0001$, *** $p < 0.001$, ** $p < 0.01$, * $p < 0.05$.

HUVEC cell viability significantly decreases at lower TNF-alpha concentrations (10-15 ng/ml), dropping to 55-65%. As the concentration increases (20-25 ng/ml), there is a gradual recovery in viability, reaching 65-80%. At higher concentrations (30-50 ng/ml), viability levels approach the baseline, ranging from 85-95%, indicating reduced toxicity or increased cell resilience at these levels.

The graph shows a significant reduction in cell viability at TNF-α concentrations of 10, 15, and 20 ng/ml, with the lowest viability (~50%) at 10 ng/ml. It is recommended to avoid these concentrations when trying to maintain HUVEC (Human

Umbilical Vein Endothelial Cells) viability, as TNF-α at these levels has a pronounced cytotoxic effect.

At 25 ng/ml, cell viability increases, suggesting that this concentration may be within a tolerable range for HUVEC cells. This concentration could be optimal for experimental purposes that require balancing cell viability with TNF-α exposure.

Interestingly, at 30 ng/ml and 50 ng/ml, cell viability increases significantly, nearly reaching control levels. This suggests a potential threshold where TNF-α toxicity diminishes, or adaptive responses in HUVEC cells become more effective at countering the inflammatory effects.

Based on the observed results, TNF-α concentrations between 25 and 30 ng/ml could be recommended for further studies, as they appear to balance cell survival with inflammatory signaling. This range could be ideal for applications that aim to maintain cell function while inducing a mild stress response.

The increase in cell viability at higher TNF-α concentrations is an interesting result that may indicate an adaptive response or reduced sensitivity to the inflammatory cytokine. Further research into the molecular mechanisms behind this recovery could provide valuable insights into endothelial cell behavior under inflammatory conditions.

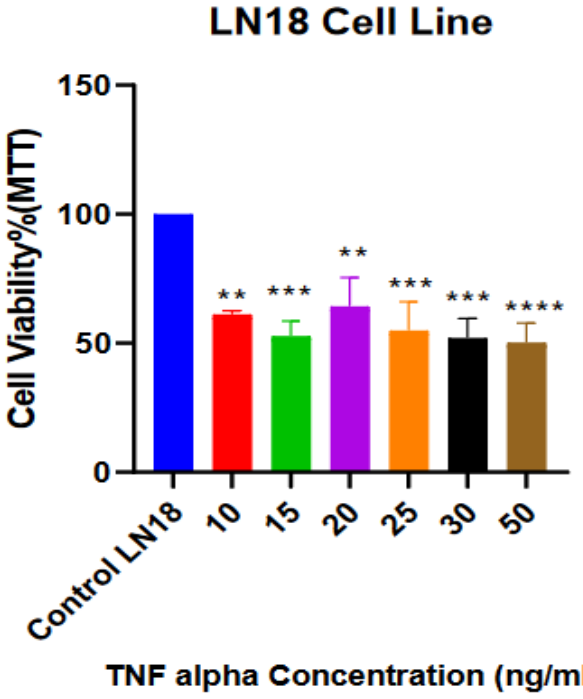

Figure 11. Cell viability percentages of LN18 with different TNF alpha concentrations. Analysis was done by one-way ANOVA, **** $p < 0.0001$, *** $p <$ 0.001, 0.01, * $p < 0.05$.

The LN18 cell line exhibits a significant decrease in viability when exposed to increasing concentrations of TNF-alpha. Viability drops from around 65-70% at 10 ng/ml to as low as 50-55% at 50 ng/ml, with the lowest viability observed at the highest concentration. Overall, TNF-alpha consistently reduces LN18 cell viability, with the most substantial impact at 50 ng/ml.

The graph shows a clear decline in the viability of the LN18 cell line as TNF-α concentrations increase. Even at the lowest concentration (10 ng/ml), the cell viability drops significantly below the control, suggesting that TNF-α has a cytotoxic effect on this cell line across all tested doses.

Among the concentrations, 20 and 25 ng/ml seem to maintain a relatively higher viability (~60%) compared to other concentrations. For experiments where some cell survival is necessary, these concentrations might be more appropriate, though viability is still markedly reduced.

At TNF-α concentrations of 30 and 50 ng/ml, cell viability decreases further, with the lowest viability (~40%) observed at 50 ng/ml. These concentrations are highly

cytotoxic for LN18 cells, and should be avoided in applications where cell survival is crucial.

For studies aiming to explore the effects of TNF-α on LN18 cells without inducing excessive cell death, concentrations around 10 to 20 ng/ml may provide a balance. However, all tested concentrations still lead to a significant reduction in cell viability, so caution is advised.

The strong cytotoxic effect of TNF-α on the LN18 cell line suggests its potential use in combination with other therapies targeting glioblastoma, as TNF-α could induce significant cell death in this cancer cell type.

The pronounced decrease in viability across all concentrations indicates that TNF-α may activate specific cell death pathways in LN18 cells. Further investigation into these mechanisms could provide insights into how TNF-α could be used in therapeutic contexts.

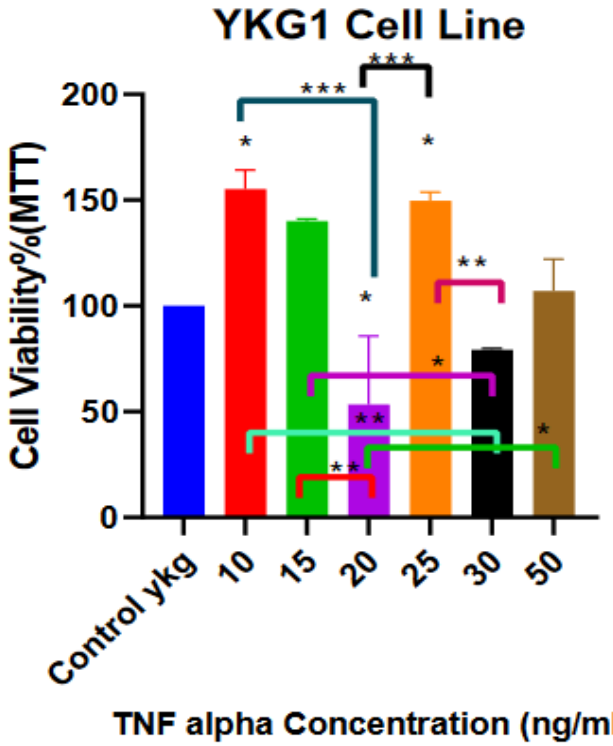

Figure 12. Cell viability percentages of YKG1 with different TNF alpha concentrations. Analysis was done by one-way ANOVA, **** $p < 0.0001$, *** $p < 0.001$, 0.01, * $p < 0.05$.

The YKG1 cell line shows a biphasic response to TNF-alpha. At lower concentrations (10-15 ng/ml), cell viability increases significantly, peaking at around 160-170% at 10 ng/ml. However, at 20 ng/ml, viability sharply drops to 70-75%, followed by a partial recovery at 25 ng/ml (130-140%). At higher concentrations (30-50 ng/ml), viability decreases. This indicates that while low concentrations of TNF-alpha promote cell proliferation, higher concentrations are toxic to the cells.

The graph shows that at 10 and 15 ng/ml, the YKG1 cell line exhibits significantly increased viability, with a peak around 150-170% compared to the control. These concentrations may be optimal for applications where promoting cell growth or survival is desirable.

At 20 ng/ml, there is a notable drop in viability (around 50%), indicating that this concentration induces significant cytotoxicity. However, at 25 ng/ml, cell viability increases again, suggesting a complex, dose-dependent response. This indicates that further investigation is needed to understand the threshold between toxicity and viability at these intermediate levels.

At 30 and 50 ng/ml, the viability drops significantly, with values around 50% of the control. These concentrations are strongly cytotoxic for YKG1 cells and should be considered for experiments aiming to induce cell death.

The asterisks marking statistical significance (*) across various concentrations highlight the importance of these findings. The most significant decreases are seen between the lower (10-15 ng/ml) and higher concentrations (20-50 ng/ml), suggesting that TNF-α induces clear, dose-dependent cytotoxic effects at higher doses. For applications requiring maintenance or promotion of YKG1 cell survival, TNF-α concentrations of 10-15 ng/ml are recommended. This range stimulates cell growth, as indicated by the increased viability percentages. For experiments focused on inducing cell death, concentrations above 25 ng/ml are recommended, as these significantly reduce cell viability. The steep decline in cell survival at 30 and 50 ng/ml makes them ideal for cytotoxicity studies. The variability in responses at 20 and 25 ng/ml suggests that this concentration range warrants further exploration to better understand the mechanisms causing such shifts between reduced and increased viability.

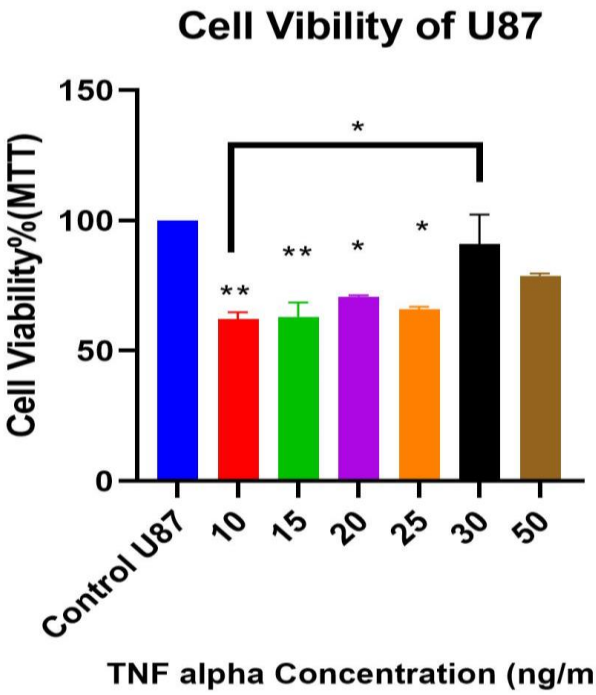

Figure 13. Cell viability percentages of U87 with different TNF alpha concentrations. Analysis was done by one-way ANOVA, **** $p < 0.0001$, *** $p <$ 0.001, 0.01, * $p < 0.05$.

At TNF-α concentrations of 10, 15, and 20 ng/ml, U87 cell viability drops to about 60-70% of the control, as indicated by the double and single asterisks for statistical significance. These concentrations induce notable cytotoxicity and could be useful in experiments where a reduction in U87 cell survival is required.

Cell viability remains low at 25 ng/ml, hovering around 70% of the control. This concentration still exerts a cytotoxic effect but shows a slight recovery compared to lower concentrations. It may be useful for balancing cell death with residual survival.

At concentrations of 30 and 50 ng/ml, cell viability rebounds close to 100%, similar to the control group. This indicates that higher concentrations of TNF-α may not induce further cytotoxic effects and could instead promote cell survival mechanisms or adaptation to the stressor.

TNF-α concentrations between 10-20 ng/ml are recommended for experiments aiming to reduce U87 cell viability. These doses show a significant reduction in cell survival and are effective at inducing cytotoxicity.

The increase in viability at 30-50 ng/ml indicates that U87 cells may adapt or trigger survival pathways at higher TNF-α concentrations. These concentrations could be explored in studies focusing on cell resistance mechanisms to TNF-α or stress adaptation.

The graph suggests a transition in cell response around 25-30 ng/ml, where cytotoxicity decreases and survival begins to recover. This concentration range might be useful for studying the shift in cellular responses from stress-induced death to potential survival or adaptation.

U87 cells show a concentration-dependent response to TNF-α, with lower doses leading to cytotoxicity and higher doses showing potential survival mechanisms. Researchers should adjust TNF-α concentrations based on whether the goal is to reduce viability or explore stress adaptation pathways.

4.3 MTT Cell Viability Analysis of Different Treatment Groups

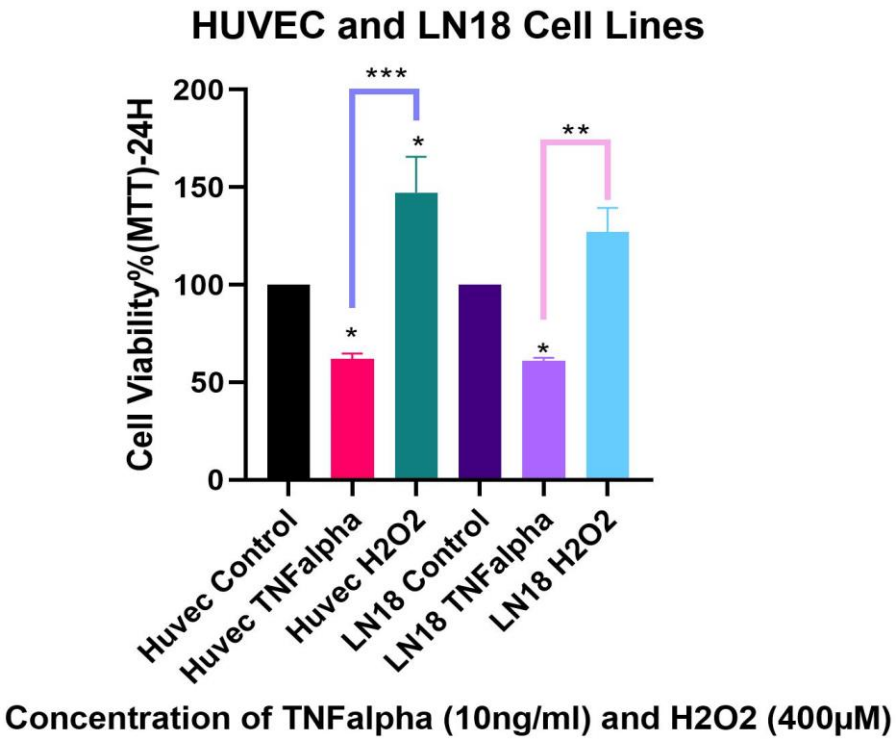

Figure 14. Cell viability percentages of HUVEC and LN18 with different treatment groups in 24 hours. Analysis was done by one-way ANOVA, **** $p < 0.0001$, *** $p < 0.001$, ** $p < 0.01$, * $p < 0.05$.

HUVEC Cells Respond Better to H_2O_2 than TNF-α Alone: The HUVEC cell viability significantly increases (~160%) when treated with 400 μM of H_2O_2 compared to the control, indicating that H_2O_2 has a stimulatory effect on HUVEC cells. However, treatment with TNF-α (10 ng/ml) decreases the cell viability to ~50%, suggesting that TNF-α has a cytotoxic effect on HUVEC cells. It is recommended to use H_2O_2 over TNF-α for experiments aimed at promoting HUVEC viability.

Combination of H_2O_2 with TNF-α Could Mitigate TNF-α Cytotoxicity in HUVEC: Given the significant increase in viability with H_2O_2 treatment, it could explore whether H_2O_2 can mitigate the cytotoxic effects of TNF-α when used in combination. This could provide insights into potential protective mechanisms in endothelial cells under inflammatory stress.

In LN18 cells, both TNF-α and H_2O_2 treatments lead to reduced cell viability compared to the HUVEC control, with TNF-α reducing viability to ~50% and H_2O_2 leading to a slight recovery (~130%). This suggests that while both treatments have a cytotoxic effect, H_2O_2 may still provide some level of cell viability improvement compared to TNF-α alone. Further exploration of dosage or combination treatments may be necessary to enhance therapeutic effects while reducing cytotoxicity.

The differential response between HUVEC and LN18 cells suggests that distinct strategies should be employed depending on the cell type. For HUVEC cells, H_2O_2 shows promise for enhancing cell viability, whereas for LN18 cells, TNF-α alone appears to be a more effective agent for reducing viability, potentially useful for anti-cancer strategies.

Since HUVEC cells show increased viability with H_2O_2 but not TNF-α, while LN18 cells show reduced viability with TNF-α and slight recovery with H_2O_2, exploring a combination of these agents in different dosing regimens could help to refine therapeutic approaches. This might lead to more selective targeting of cell types based on their specific vulnerabilities.

These recommendations suggest that H_2O_2 may enhance endothelial cell survival, while TNF-α may serve as a more potent cytotoxic agent in cancer cell lines like LN18. The response variability highlights the importance of tailored treatments based on cell type.

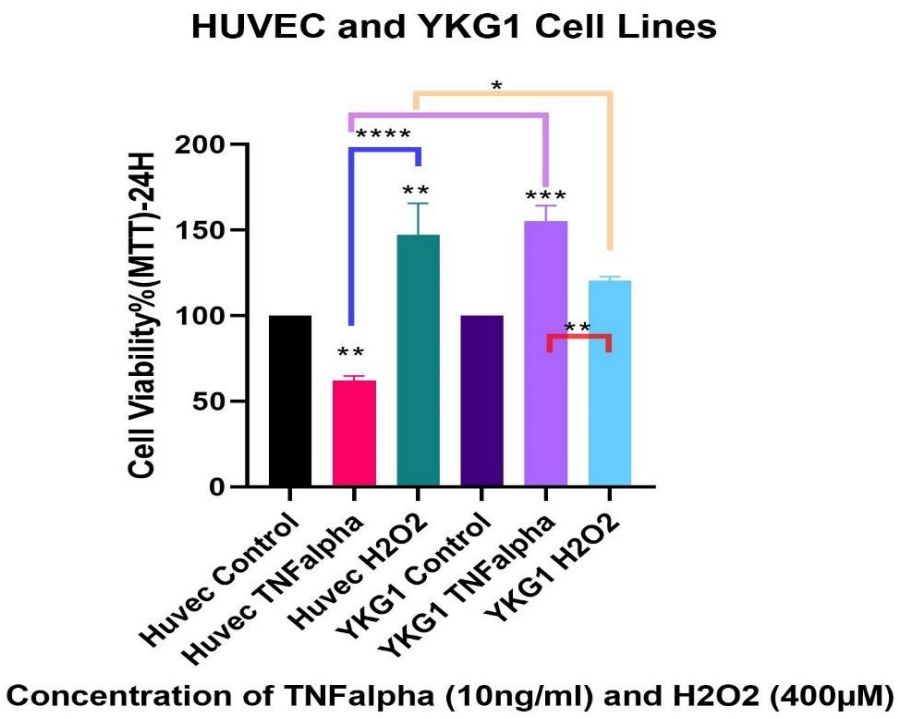

Figure 15. Cell viability percentages of HUVEC and YKG1 with different treatment groups in 24 hours. Analysis was done by one-way ANOVA, **** $p < 0.0001$, *** $p < 0.001$, ** $p < 0.01$, * $p < 0.05$.

Treatment of HUVEC cells with 400 µM H_2O_2 significantly increases viability to approximately 175%, as indicated by the quadruple asterisks (****). This suggests a protective or stimulatory effect of H_2O_2 on HUVEC cells. H_2O_2 could be a potential agent to promote HUVEC viability, making it suitable for studies focusing on endothelial cell proliferation or survival. TNF-α (10 ng/ml) significantly reduces HUVEC cell viability to below 50%, marked by double asterisks (**). TNF-α alone has a strong cytotoxic effect on these cells. For inducing cytotoxicity or mimicking inflammatory conditions in HUVEC cells, TNF-α should be utilized. However, caution is needed if cell survival is required. In contrast to HUVEC, TNF-α increases YKG1 cell viability to about 150%, indicating a potentially stimulatory effect on these cells. TNF-α may have a pro-survival effect on YKG1 cells, and further research into this response could uncover important mechanisms in tumor cell adaptation to inflammatory environments. It is a useful agent for studies on cell proliferation in glioblastoma. H_2O_2 increases YKG1 cell viability to about 140%, similar to TNF-α, indicating that oxidative stress enhances survival or proliferation in YKG1 cells.

H_2O_2 is beneficial for studies aiming to increase YKG1 cell viability. However, the combined effects of oxidative stress and inflammatory signals (like TNF-α) should be explored for their potential in driving tumor cell proliferation. Both HUVEC and YKG1 cells exhibit different responses to H_2O_2 and TNF-α treatments, showing increased viability in the YKG1 glioblastoma line and decreased viability in HUVEC cells with TNF-α. Meanwhile, H_2O_2 stimulates viability in both cell lines, though more significantly in HUVEC. Explore combined or sequential treatments using H_2O_2 and TNF-α to investigate differential responses in tumor versus endothelial cells. Such treatments could provide insights into selective targeting strategies for cancer therapy.

HUVEC cells benefit from H_2O_2 but are sensitive to TNF-α-induced cytotoxicity. YKG1 cells show increased viability in response to both H_2O_2 and TNF-α, suggesting potential tumor-promoting effects of these agents. Depending on the cell type, H_2O_2 and TNF-α can either promote survival or induce cytotoxicity, making these agents valuable for tailored experiments focusing on cancer versus normal cell responses.

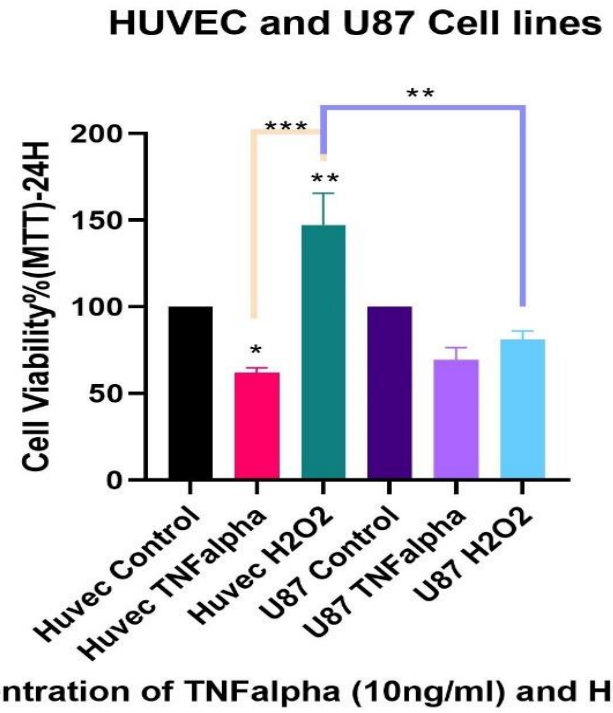

Figure 16. Cell viability percentages of HUVEC and U87 with different treatment groups in 24 hours. Analysis was done by one-way ANOVA, **** $p < 0.0001$, *** $p < 0.001$, ** $p < 0.01$, * $p < 0.05$.

According to the Graph: In U87 cells, TNF-α decreases cell viability to around 60%, while H_2O_2 treatment maintains cell viability close to control levels (around 90%). TNF-α can be used to reduce U87 cell viability for glioblastoma-related cytotoxicity studies, while H_2O_2 appears to have a minimal impact on U87 cells and may not be effective for inducing significant cytotoxicity in these cancer cells. The different responses of HUVEC and U87 cells to TNF-α and H_2O_2 highlight the contrasting effects of these agents on endothelial versus cancer cell lines. While TNF-α is cytotoxic to both, H_2O_2 enhances HUVEC viability and has little effect on U87 cells.

The results suggest that combining TNF-α and H_2O_2 could be explored, particularly to reduce cytotoxicity in non-cancerous cells like HUVEC while selectively targeting cancerous cells like U87.It could focus on the combined effects of TNF-α and H_2O_2 in mixed cell environments to explore selective therapeutic approaches. The differential effects of H_2O_2 and TNF-α on endothelial and cancer cells, providing valuable insights for targeted experimental design.

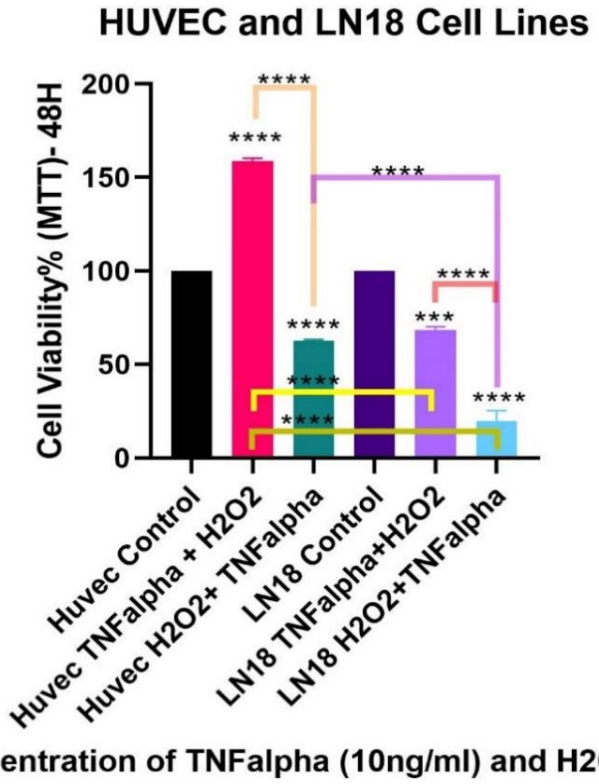

Figure 17. Cell viability percentages of HUVEC and LN18 with different treatment groups in 48 hours. Analysis was done by one-way ANOVA, **** $p < 0.0001$, *** $p < 0.001$, ** $p < 0.01$, * $p < 0.05$.

HUVEC cells seem highly sensitive to oxidative stress (H_2O_2) when combined with TNF-alpha, showing almost complete loss of viability. In LN18 cells, while both oxidative stress (H_2O_2) and inflammatory cytokine (TNF-alpha) treatments reduce viability, the combination is even more effective. This suggests potential avenues for combination therapies targeting glioblastoma cells through both oxidative stress and inflammation pathways.

The synergy between TNF-alpha and H_2O_2 in both HUVEC and LN18 cells points toward the importance of combined treatment approaches, particularly for conditions like cancer or vascular diseases, where both oxidative and inflammatory stressors are common. The increased viability in HUVEC cells with TNF-alpha alone suggests TNF-alpha may promote proliferation or survival pathways in certain cell types, particularly in endothelial cells, which might have implications in diseases involving vascular proliferation, like cancer or atherosclerosis.

This analysis suggests that oxidative and inflammatory stresses have profound effects on cell viability, and their combination may serve as a powerful tool in developing therapeutic approaches for diseases like glioblastoma.

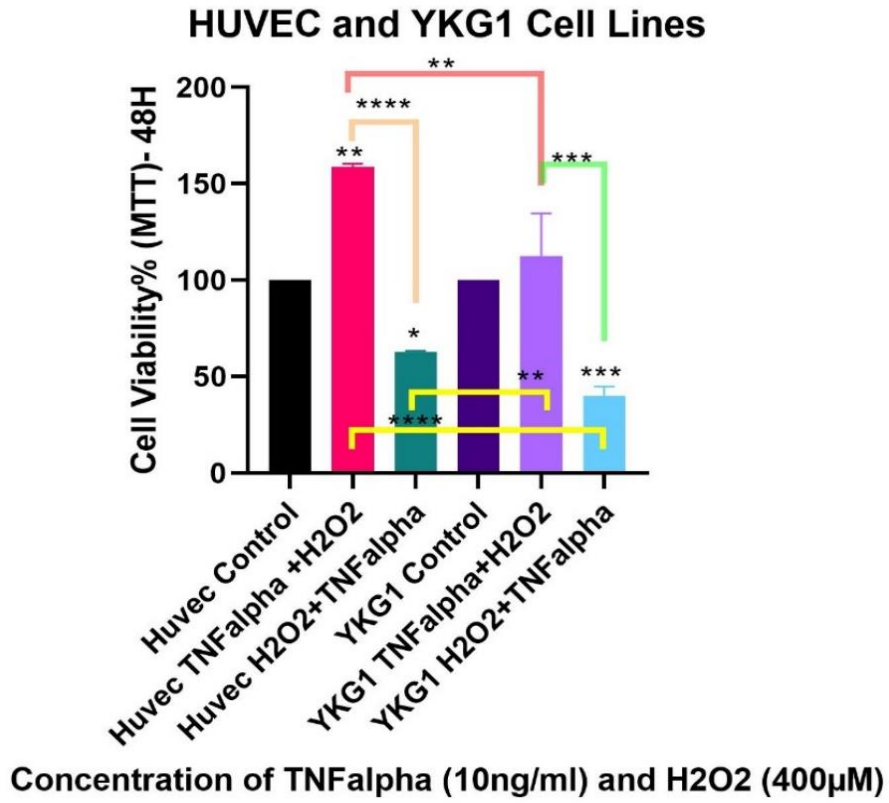

Figure 18. Cell viability percentages of HUVEC and YKG1 with different treatment groups in 48 hours. Analysis was done by one-way ANOVA, **** $p < 0.0001$, *** $p < 0.001$, ** $p < 0.01$, * $p < 0.05$.

YKG1 cells show reduced viability in response to H_2O_2 + TNF-alpha, with the combination of these agents being particularly cytotoxic. This suggests a potential for combination therapies targeting both inflammatory and oxidative stress pathways in glioma or other cancer types. The observation that TNF-alpha + H_2O_2 boosts HUVEC viability significantly could be indicative of an adaptive or proliferative response to inflammation in endothelial cells. This effect could have implications for diseases involving vascular inflammation, such as atherosclerosis or cancer.

The cytotoxic effects seen in YKG1 cells with H_2O_2 + TNF-alpha treatments suggest that glioma cells may be particularly vulnerable to combined inflammatory and oxidative stress, providing a potential strategy for targeting glioma cells in therapy.

Given the combined cytotoxic effects of TNF-alpha and H_2O_2 in both cell lines, a combined approach targeting both inflammation and oxidative stress could offer promising therapeutic benefits in treating cancers or other diseases involving these pathways. This analysis suggests that oxidative and inflammatory stresses have a profound impact on cell viability, particularly when combined, offering insights into how these stressors could be leveraged in therapeutic strategies.

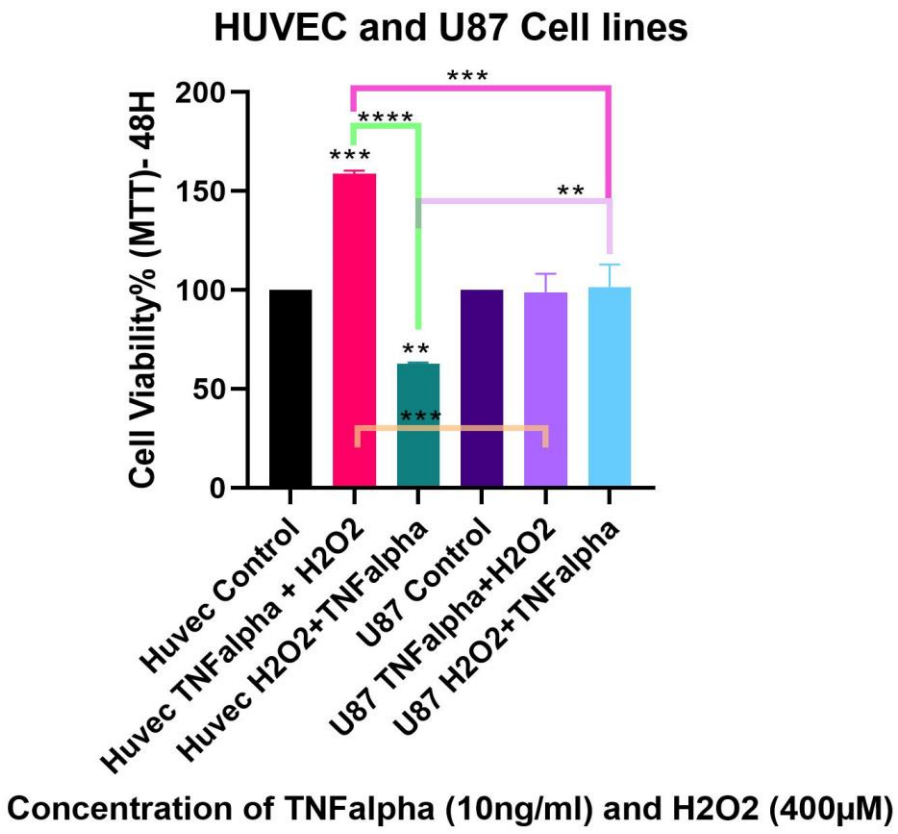

Figure 19. Cell viability percentages of HUVEC and U87 with different treatment groups in 48 hours Analysis was done by one-way ANOVA, **** $p < 0.0001$, *** $p < 0.001$, ** $p < 0.01$, * $p < 0.05$.

U87 cells demonstrate resistance to combination of the oxidative stress (H_2O_2) and inflammatory (TNF-alpha). This suggests that glioblastoma cells like U87 may have protective mechanisms that allow them to withstand such stress, making them harder to target through these pathways.

U87 glioblastoma cells are resistant to TNF-alpha and H_2O_2 -induced stress, therapies targeting other pathways may be more effective. Combination therapies that disrupt these cells' resistance mechanisms could be explored for more effective treatment strategies.

This analysis highlights the differential sensitivity of endothelial and glioblastoma cells to inflammatory and oxidative stress.

4.4 ROS Level Analysis of Different Treatment Groups

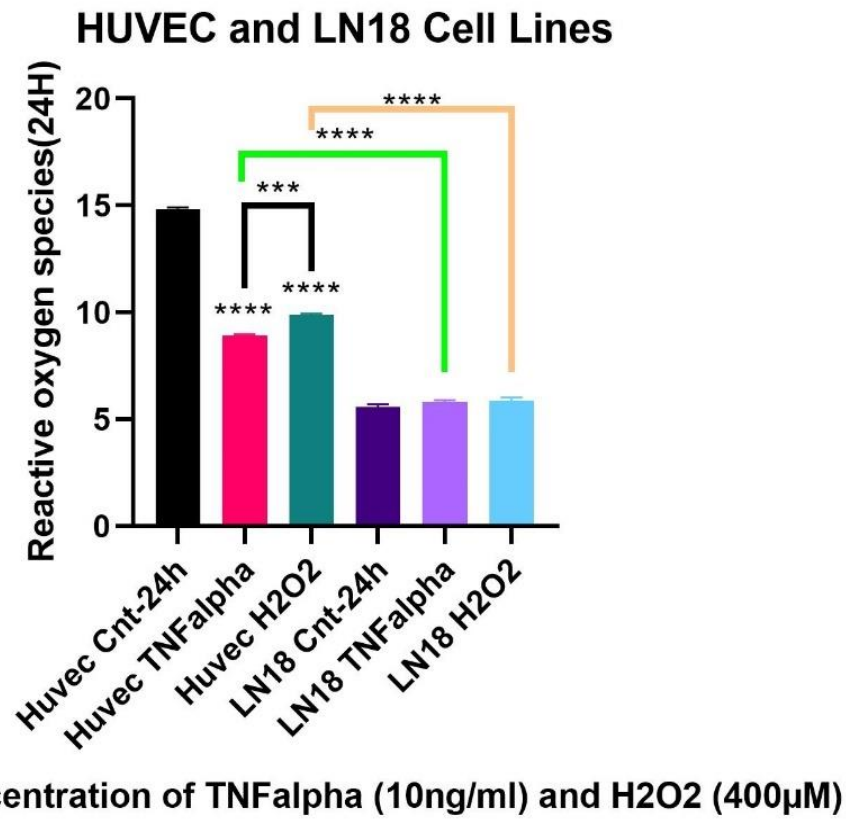

Figure 20. ROS level of HUVEC and LN18 with different treatment groups in 24 hours. Analysis was done by one-way ANOVA, **** $p < 0.0001$, *** $p < 0.001$, ** $p < 0.01$, * $p < 0.05$.

According to graph, the high baseline ROS production in HUVECs could indicate a natural oxidative stress response in endothelial cells, which are often exposed to fluctuating environmental conditions (e.g., oxygen levels, shear stress). TNF-alpha appears to reduce ROS production in HUVECs, which may suggest that

TNF-alpha induces cellular responses that lower oxidative stress, possibly through the upregulation of antioxidant defenses. This finding could be explored further in anti-inflammatory strategies that aim to modulate ROS levels.

The minimal change in ROS levels in LN18 glioblastoma cells, even after exposure to TNF-alpha and H_2O_2, suggests that these cells may have efficient ROS-scavenging mechanisms or are resistant to oxidative stress-induced ROS production. This could explain the resilience of glioblastoma cells to certain stressors and may point to the need for alternative therapeutic approaches that target other vulnerabilities in these cells. The reduction in ROS production after H_2O_2 treatment in HUVEC cells might indicate a paradoxical activation of protective responses, such as the upregulation of antioxidant enzymes like superoxide dismutase or catalase. Investigating these mechanisms could provide insights into how endothelial cells manage oxidative stress.

For HUVEC cells, strategies that either modulate ROS levels or target the antioxidant systems may offer a way to protect endothelial cells from damage in inflammatory or oxidative stress conditions. For LN18 cells, alternative approaches may be needed, given their resistance to changes in ROS levels under the tested conditions.

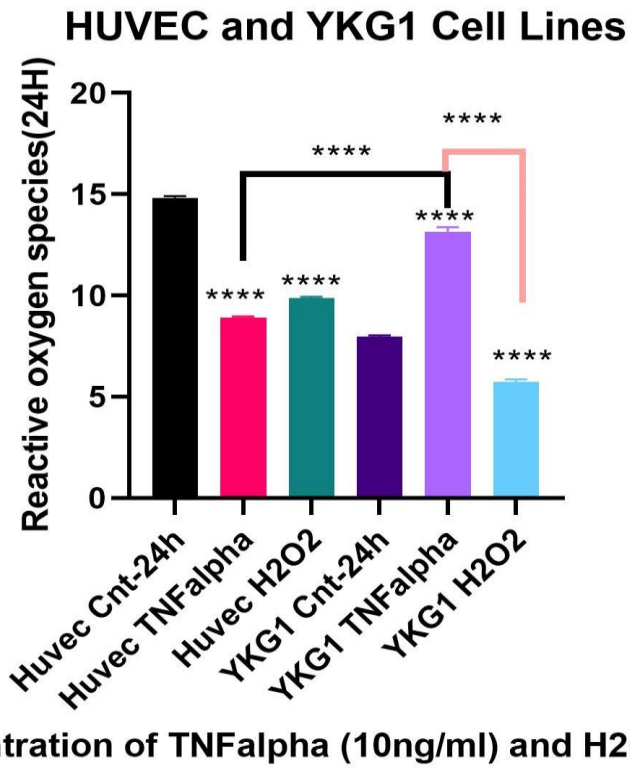

Figure 21. ROS level of HUVEC and YKG1 with different treatment groups in 24 hours. Analysis was done by one-way ANOVA, **** $p < 0.0001$, *** $p < 0.001$, ** $p < 0.01$, * $p < 0.05$.

The significant increase in ROS in YKG1 cells after TNF-alpha treatment suggests that inflammation induces oxidative stress in these cells. This may make YKG1 cells more susceptible to oxidative damage under inflammatory conditions, offering a potential therapeutic target in cancer treatment.

The decrease in ROS levels in YKG1 cells after H_2O_2 treatment may indicate that these cells have an effective antioxidant response. This resilience to oxidative stress could contribute to the survival and proliferation of cancer cells under stress conditions. Therapies that target the antioxidant pathways in YKG1 cells could be explored to overcome this resistance. While HUVECs show a consistent reduction in ROS under both TNF-alpha and H_2O_2 treatments, YKG1 cells respond differently, with TNF-alpha increasing ROS and H_2O_2 decreasing it. This suggests that the two cell types manage oxidative and inflammatory stress in distinct ways, which could be leveraged in the development of targeted treatments for cancer or vascular diseases.

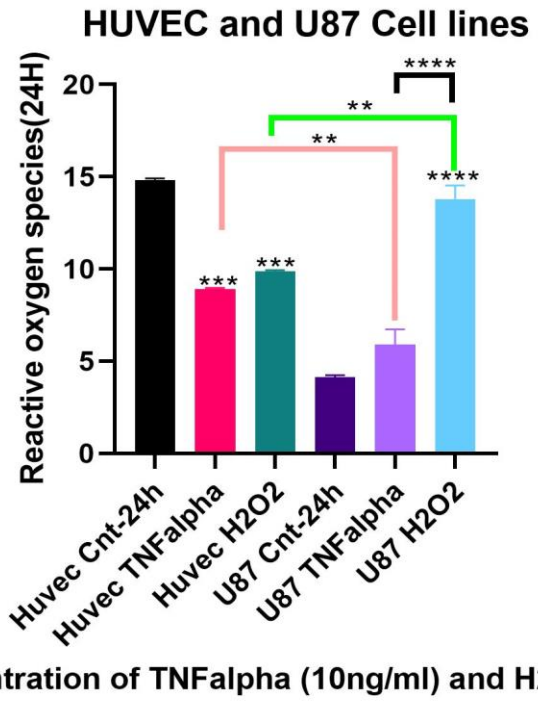

Figure 22. ROS level of HUVEC and U87 with different treatment groups in 24 hours. Analysis was done by one-way ANOVA, **** $p < 0.0001$, *** $p < 0.001$, ** $p < 0.01$, * $p < 0.05$.

U87 cells show a significant increase in ROS levels after H_2O_2 treatment, indicating a strong oxidative stress response. This suggests that glioblastoma cells may be vulnerable to treatments that increase oxidative stress, making oxidative therapies, such as ROS-inducing agents, a potential strategy for glioblastoma treatment. The lack of significant ROS production in U87 cells after TNF-alpha treatment may indicate that glioblastoma cells are resistant to inflammatory-induced ROS or possess mechanisms to buffer oxidative damage from inflammation. This highlights the importance of considering alternative pathways, other than ROS generation, when targeting inflammation in glioblastoma.

The stark difference in ROS responses between HUVEC and U87 cells suggests that these cell types handle oxidative and inflammatory stress very differently. Therapeutic strategies could exploit the increased ROS vulnerability of U87 cells, while approaches for endothelial cells like HUVEC might focus on bolstering their antioxidant defenses. HUVEC cells show reduced ROS levels under both TNF-alpha and H_2O_2, suggesting a strong antioxidant response. U87 glioblastoma cells are more

resistant to TNF-alpha-induced ROS but highly susceptible to H_2O_2 -induced oxidative stress. These findings indicate that targeting oxidative stress could be more effective in glioblastoma treatment, while managing ROS in endothelial cells requires a different approach.

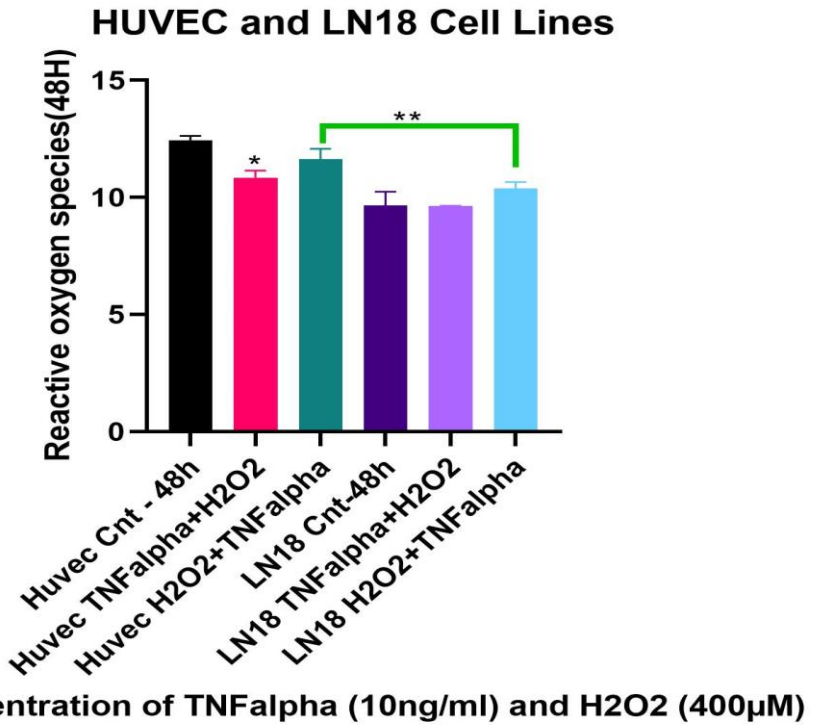

Figure 23. ROS level of HUVEC and LN18 with different treatment groups in 48 hours. Analysis was done by one-way ANOVA, **** $p < 0.0001$, *** $p < 0.001$, ** $p < 0.01$, * $p < 0.05$.

HUVEC cells demonstrate a slight decrease in ROS after both TNF-alpha and H_2O_2 treatments, suggesting that these cells activate protective antioxidant mechanisms in response to stress. LN18 cells show a lower baseline ROS production compared to HUVECs and minimal changes in ROS levels after TNF-alpha and H_2O_2 treatments. This could indicate that LN18 glioblastoma cells are less sensitive to oxidative stress or that they possess efficient ROS management systems. Therapeutic approaches that target other vulnerabilities in glioblastoma cells, such as disrupting their ROS regulation, may be necessary.

Both HUVEC and LN18 cells show a similar pattern of ROS reduction or minimal changes with the combination of TNF-alpha and H_2O_2. This suggests that

oxidative and inflammatory stress, when combined, might trigger protective mechanisms that counteract ROS production in both cell lines. Understanding these protective responses could offer insights into potential therapeutic targets. HUVEC cells show a slight reduction in ROS with TNF-alpha and H_2O_2, indicating a robust antioxidant response. LN18 cells maintain low ROS levels, showing resistance to oxidative stress. Therapeutic strategies could focus on enhancing antioxidant defenses in endothelial cells like HUVEC or targeting ROS regulation mechanisms in glioblastoma cells like LN18.

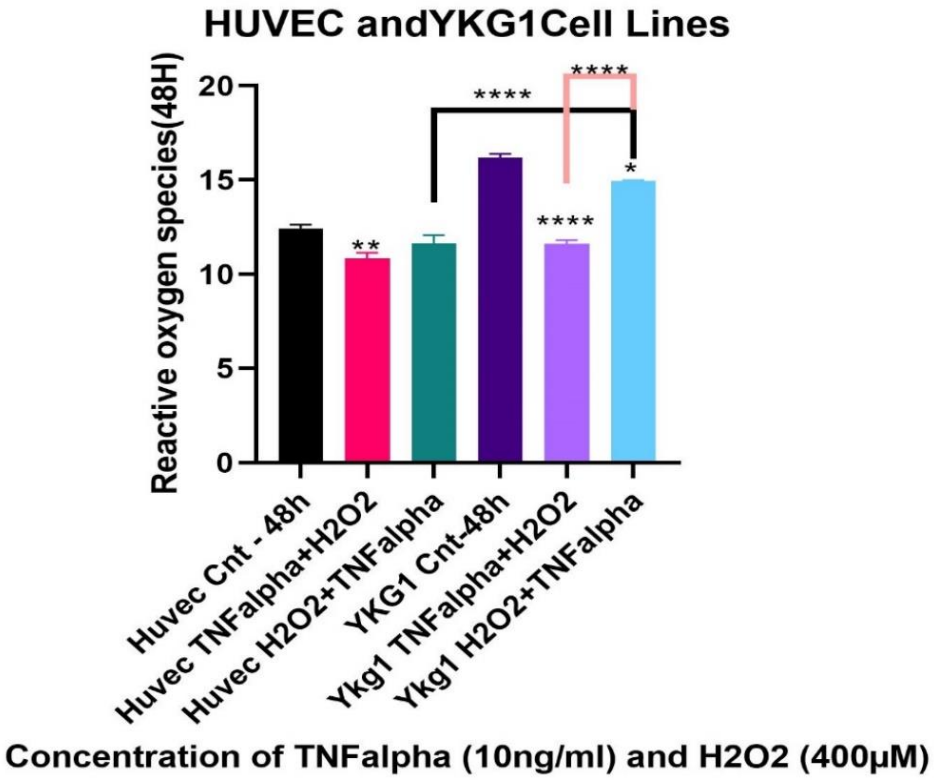

Figure 24. ROS level of HUVEC and YKG1 with different treatment groups in 48 hours. Analysis was done by one-way ANOVA, **** $p < 0.0001$, *** $p < 0.001$, ** $p < 0.01$, * $p < 0.05$.

YKG1 cells, likely a cancer cell line, show a significant increase in ROS levels in response to H_2O_2 + TNF-alpha compare to HUVEC. This heightened sensitivity to oxidative stress could be exploited in cancer treatments that induce ROS accumulation to target cancer cells. For HUVEC cells, strategies that enhance their natural antioxidant responses may be beneficial in managing diseases involving endothelial

dysfunction. In contrast, for YKG1 cells, approaches that induce oxidative stress, potentially by combining inflammatory and oxidative agents, could be an effective therapeutic strategy against cancer.

The differential ROS response between HUVEC and YKG1 cells highlights that endothelial cells and cancer cells manage oxidative and inflammatory stress very differently. These findings could inform therapeutic strategies tailored to the specific vulnerabilities of each cell type.

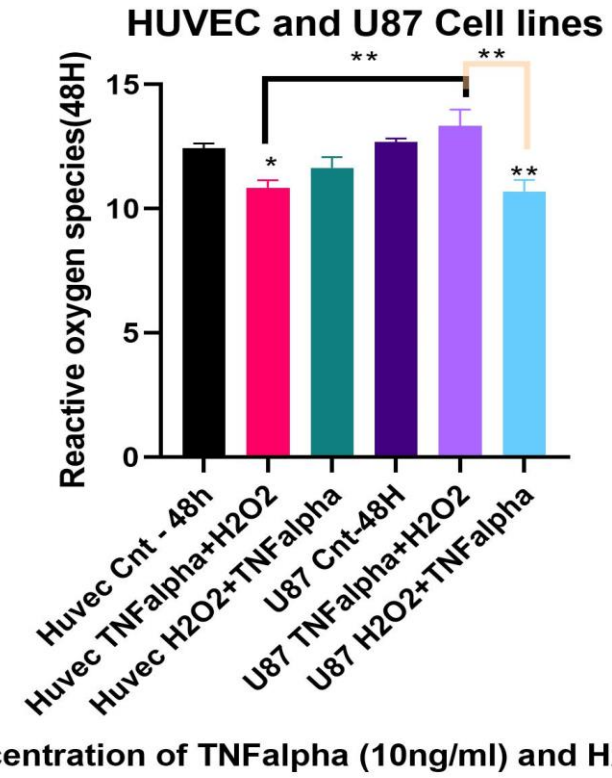

Figure 25. ROS level of HUVEC and U87 with different treatment groups in 48 hours. Analysis was done by one-way ANOVA, **** $p < 0.0001$, *** $p < 0.001$, ** $p < 0.01$, * $p < 0.05$.

U87 cells show a significant increase in ROS levels after the combination of TNF-alpha + H_2O_2, suggesting that glioblastoma cells are more vulnerable to oxidative stress. This could be exploited in cancer therapies aimed at inducing oxidative damage to target glioblastoma cells.

For HUVEC cells, therapies that enhance their antioxidant defenses might help reduce oxidative stress and protect against cellular damage. For U87 glioblastoma

cells, inducing oxidative stress could be a potential strategy to inhibit cancer growth, particularly by combining inflammatory agents like TNF-alpha with oxidative agents like H_2O_2.

HUVEC cells show a reduction in ROS with TNF-alpha and H_2O_2 treatments, suggesting a strong antioxidant response. U87 glioblastoma cells show a significant increase in ROS, especially with combined TNF-alpha + H_2O_2, indicating susceptibility to oxidative stress.

4.5 Relative Distance Analysis of Different Treatment Groups

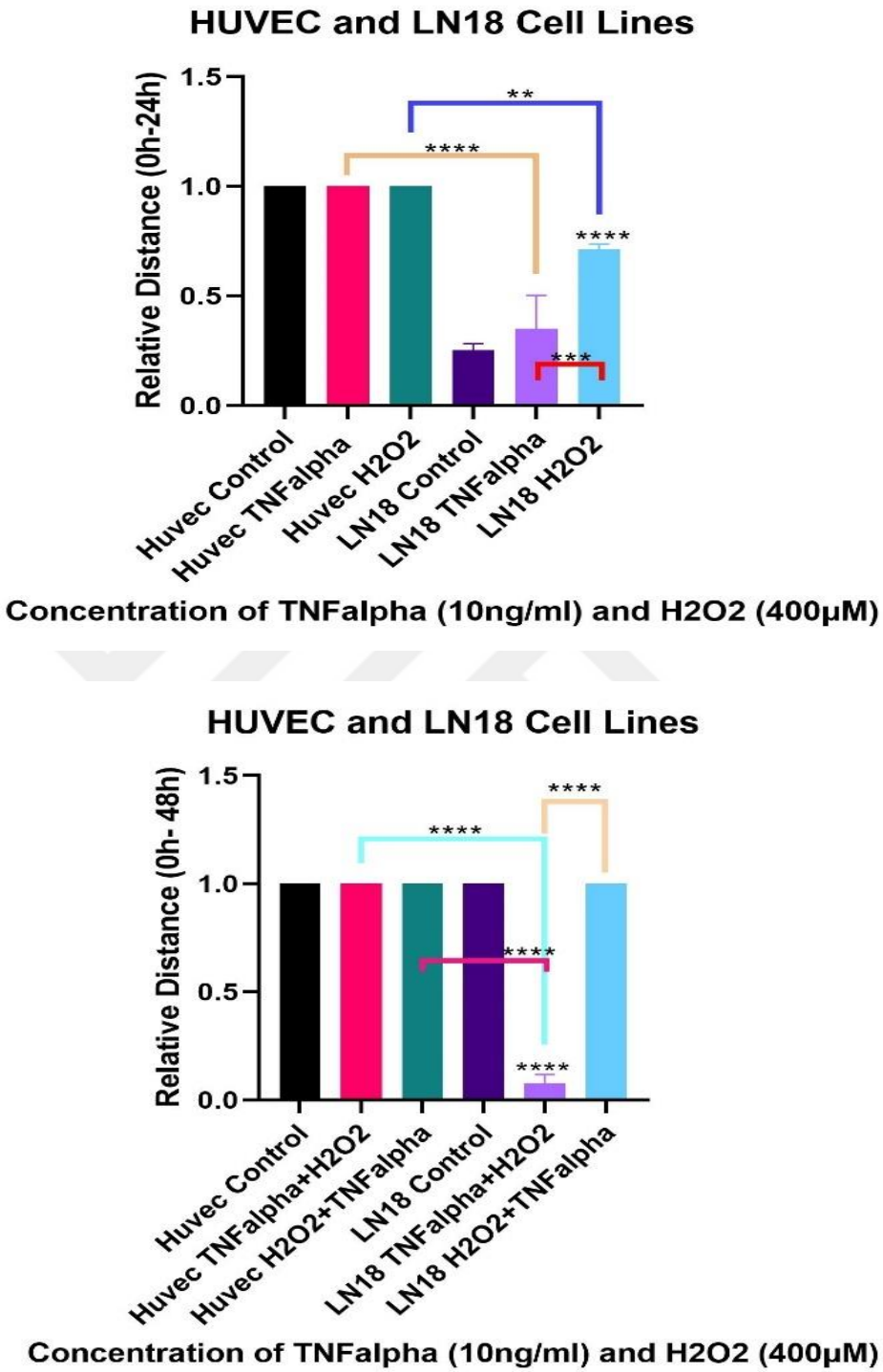

Figure 26. Relative Distance Analysis of HUVEC and LN18 with different treatment groups in 24 and 48 hours. Analysis was done by one-way ANOVA, **** $p < 0.0001$, *** $p < 0.001$, ** $p < 0.01$, * $p < 0.05$.

HUVEC cells maintain their migration ability over both 24 and 48 hours, even under TNF-alpha and H_2O_2 treatments. This suggests that endothelial cells are resistant to these stressors in terms of migration, making them more robust for wound healing or vascular repair processes.

LN18 cells show a marked reduction in migration with TNF-alpha + H_2O_2 treatments. Treatments that impair migration could potentially reduce the invasiveness and metastatic potential of glioblastoma. Since HUVEC cells are resistant to both TNF-alpha and H_2O_2 in terms of migration, therapies aiming to preserve or enhance endothelial function during inflammation or oxidative stress may not need to focus on these pathways.

HUVEC cells maintain stable migration, indicating resilience to TNF-alpha and H_2O_2 alone and combined over 24 and 48 hours. LN18 cells show impaired migration under TNF-alpha + H_2O_2, and each one alone which suggesting sensitivity to oxidative and inflammatory stress, which could be therapeutically exploited to reduce tumor invasiveness. These findings provide important insights into how endothelial and glioblastoma cells respond to stressors related to inflammation and oxidative damage.

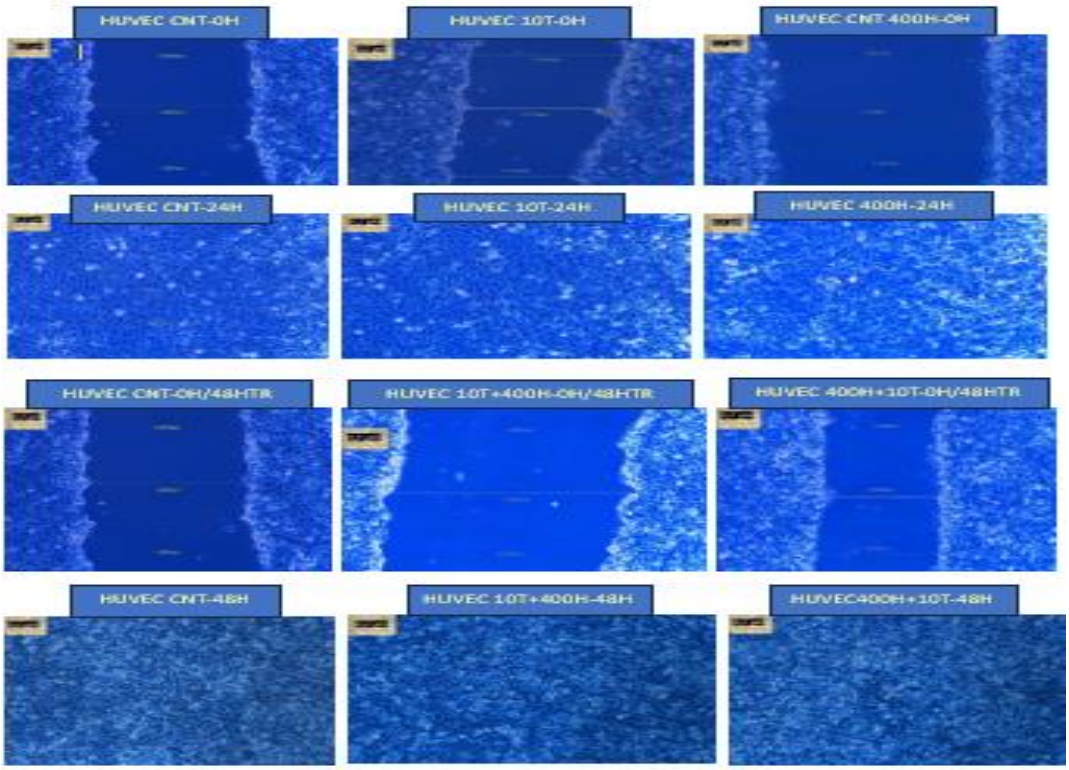

Figure 27. Scratch assay analysis of HUVEC in different treatment groups in 24 and 48 hours.

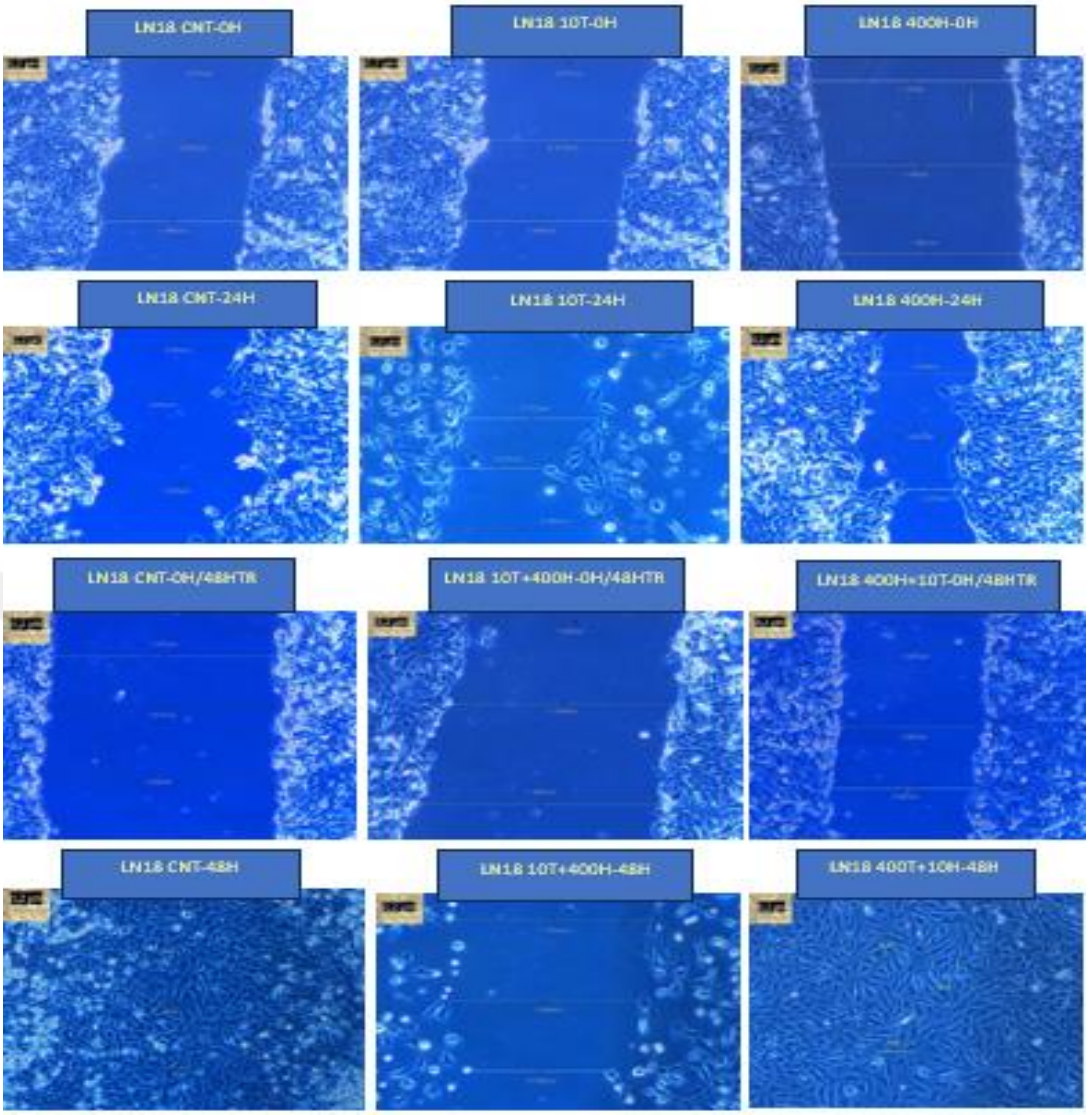

Figure 28. Scratch assay analysis of LN18 in different treatment groups in 24 and 48 hours.

The robustness of HUVEC cells against stress highlights their ability to maintain healing capacity, whereas the impairment seen in LN18 cells suggests a potential therapeutic angle to exploit in reducing cancer cell migration and invasiveness. For glioblastoma treatment, the combination of oxidative and inflammatory stress appears to significantly impair migration, suggesting that such dual therapies could help prevent tumor metastasis.

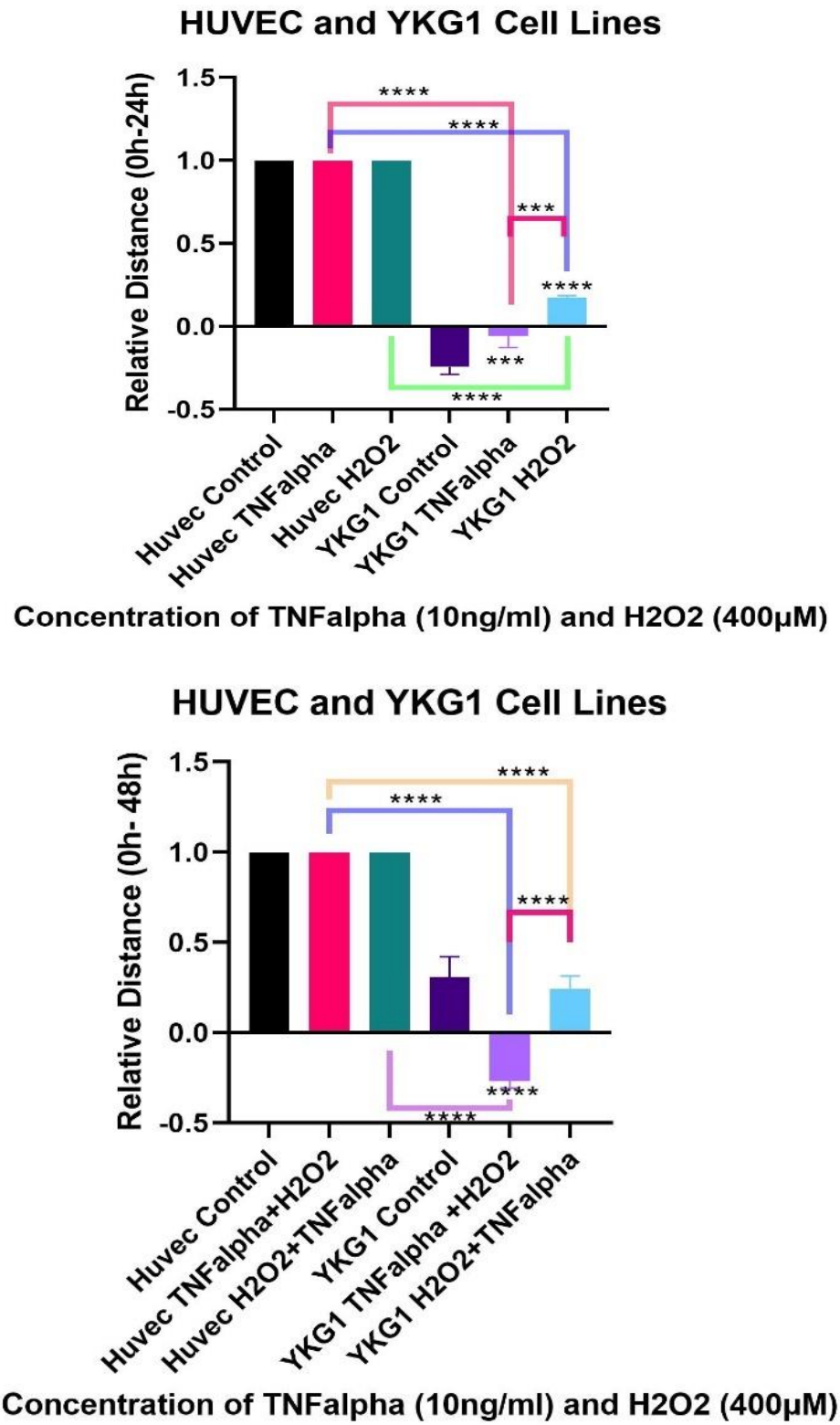

Figure 29. Relative distance analysis of HUVEC and YKG1 with different treatment groups. Analysis was done by one-way ANOVA, **** $p < 0.0001$, *** $p < 0.001$, ** $p < 0.01$, * $p < 0.05$.

YKG1 cells, show significantly reduced migration under both TNF-alpha and H_2O_2 alone and, especially with the combination treatment. This indicates that YKG1 cells are highly sensitive to oxidative and inflammatory stress, leading to impaired wound healing or migration. Targeting both oxidative and inflammatory pathways could be an effective strategy to inhibit glioblastoma or cancer cell migration. The combination of TNF-alpha and H_2O_2 could be used to impair the invasiveness of these cells.

While HUVEC cells are resistant to both TNF-alpha and H_2O_2, the combination treatment does not drastically impair migration, indicating that endothelial cells could survive inflammatory and oxidative stress conditions. The pronounced reduction in migration in YKG1 cells with the combination of TNF-alpha and H_2O_2 suggests that a dual-therapy approach could significantly impair cancer cell motility and reduce tumor spread.

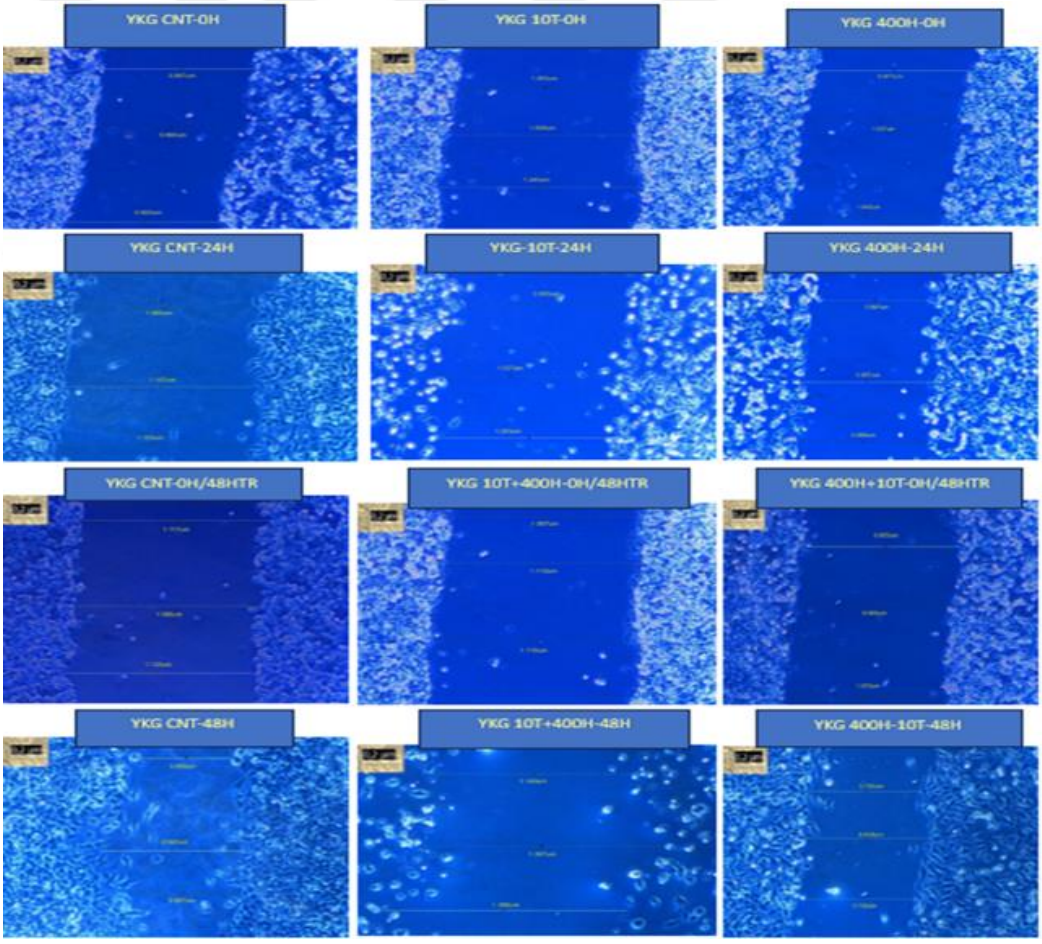

Figure 30. Scratch assay analysis of YKG1 in different treatment groups in 24 and 48 hours.

The combination of TNF-alpha and H_2O_2 shows the greatest inhibition of migration, suggesting a potential therapeutic strategy to block cancer cell invasiveness through the combined use of oxidative and inflammatory stress agents. These findings suggest that targeting oxidative and inflammatory pathways could be effective in reducing the migration and invasiveness of cancer cells such as YKG1, potentially limiting metastasis in cancers like glioblastoma.

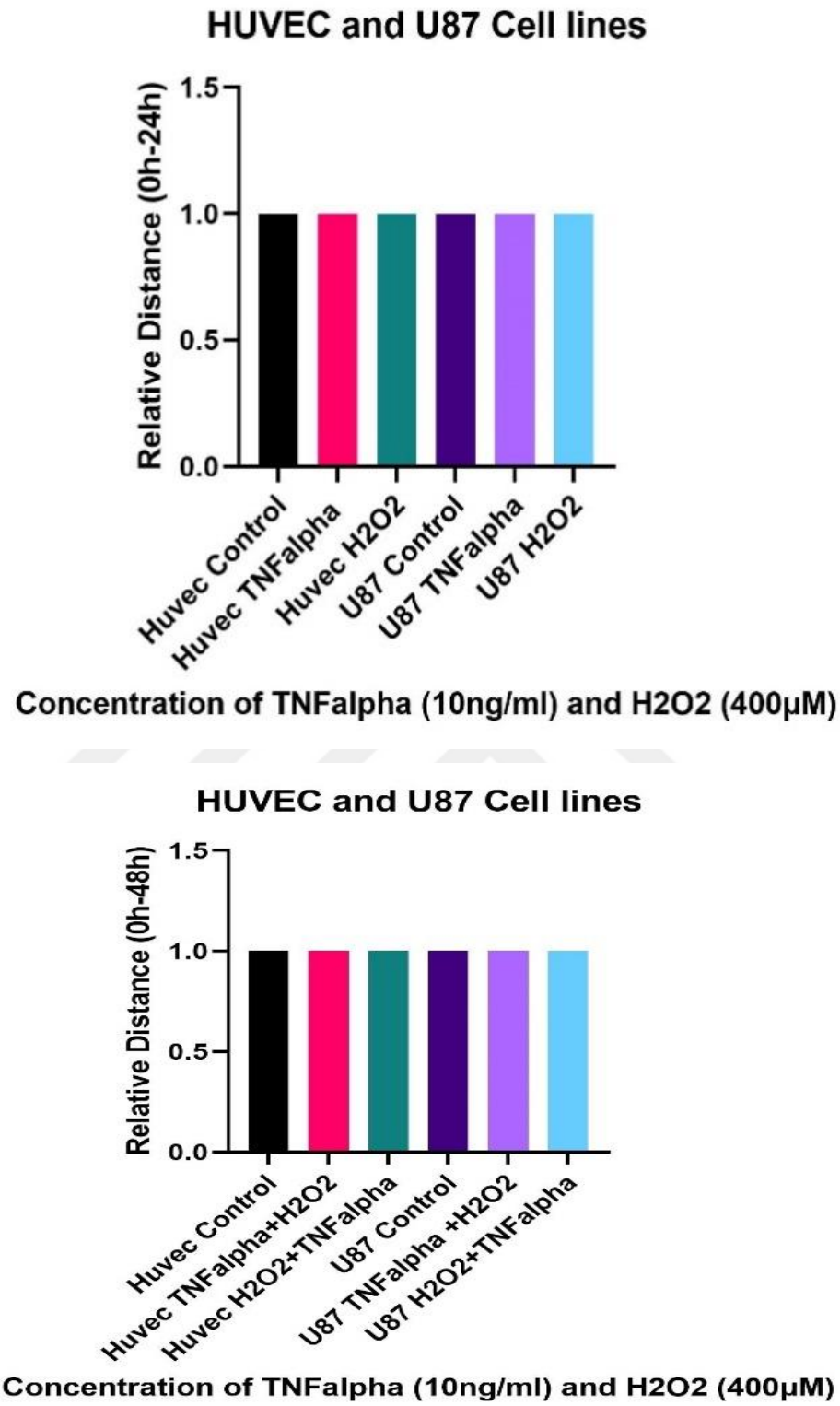

Figure 31. Relative Distance Analysis of HUVEC and U87 with different treatment groups in 24 and 48 hours. Analysis was done by one-way ANOVA, **** $p < 0.0001$, *** $p < 0.001$, ** $p < 0.01$, * $p < 0.05$.

U87 glioblastoma cells also maintain their migration capacity under TNF-alpha and H_2O_2 treatments over both 24 and 48 hours. This suggests that, like HUVEC cells, U87 cells are not significantly affected by oxidative or inflammatory stress in terms of migration.

These findings suggest that neither TNF-alpha nor H_2O_2 alone significantly impair cell migration in either endothelial or glioblastoma cells, indicating the need for different therapeutic strategies if the goal is to inhibit cancer cell movement or impair endothelial healing. These results provide valuable insights into how both cell types respond to oxidative and inflammatory stress in terms of migration, with implications for both vascular health and cancer treatment.

4.6 Scratch Assay Analysis of Different Treatment Groups

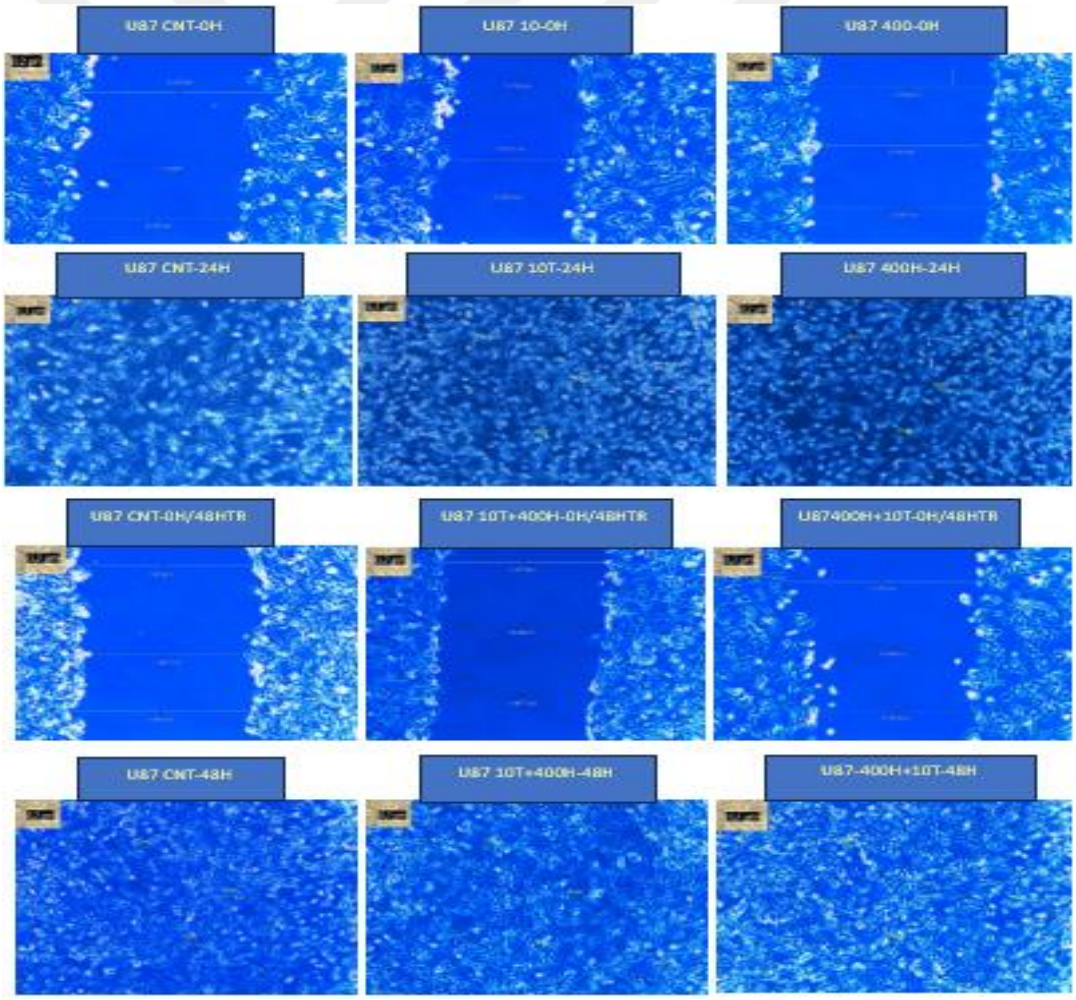

Figure 32. Scratch assay analysis of U87 in different treatment groups in 24 and 48 hours.

U87 glioblastoma cells exhibit normal migration and wound closure, with significant healing seen at 24 and 48 hours. TNF-alpha has a minimal impact on U87 cell migration, with similar wound healing rates to the control group.

Chapter 5

Discussions and Conclusions

5.1 Discussion of Findings

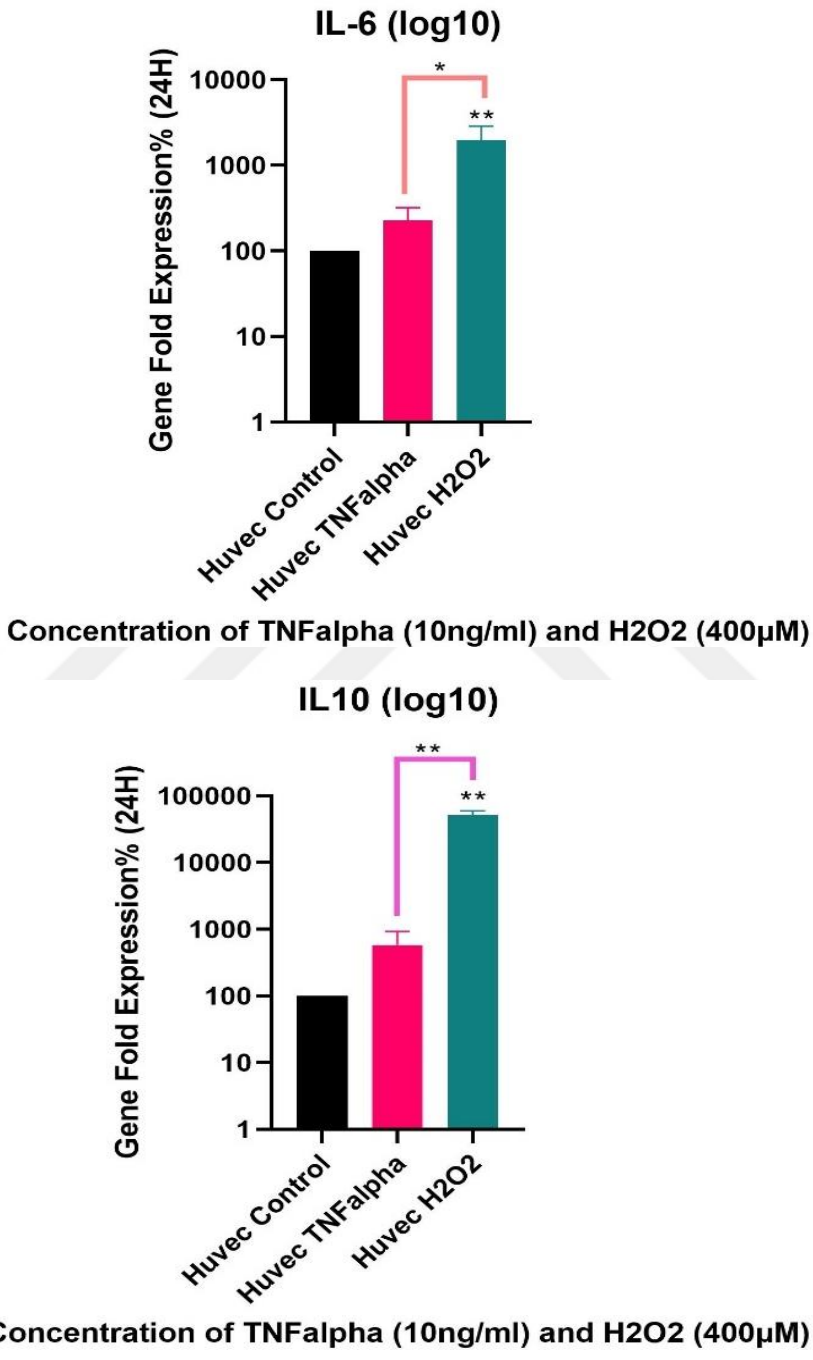

Figure 33. qRT-PCR gene fold expressions of IL-6 and IL-10 of HUVEC in 24 hours. Analysis was done by one-way ANOVA, **** $p < 0.0001$, *** $p < 0.001$, ** $p < 0.01$, * $p < 0.05$.

In the provided graphs, L-6 is a pro-inflammatory cytokine involved in the acute phase response. The data suggest that both TNF-alpha and H_2O_2 significantly upregulate IL-6 expression, with H_2O_2 having a more pronounced effect.

Since increased IL-6 is linked to inflammatory responses, oxidative stress (induced by H_2O_2) could exacerbate inflammation more than TNF-alpha alone. This could be relevant for understanding how oxidative stress influences inflammation in endothelial cells.

IL-10 is an anti-inflammatory cytokine that modulates the immune response by limiting excessive inflammation. The results show that H_2O_2 increases IL-10 expression dramatically, even more than TNF-alpha.

TNF-alpha is known to significantly increase the production of IL-6, which plays a critical role in inflammatory responses (Aggarwal et al., 2002). Additionally, oxidative stress induced by agents like H_2O_2 has been shown to exacerbate inflammatory cytokine expression, including IL-6 (Libby et al., 2002). IL-10 is an anti-inflammatory cytokine that helps modulate the immune response and control excessive inflammation (Cavaillon, 2001). Studies have demonstrated that oxidative stress may lead to the upregulation of IL-10, potentially as a compensatory mechanism to counteract increased pro-inflammatory cytokines (Nathan & Ding, 2010). H_2O_2 has been identified as a key signalling molecule in the activation of various pathways, including those responsible for cytokine regulation (Schreck et al., 1991). The balance between pro-inflammatory and anti-inflammatory cytokines, such as IL-6 and IL-10, can be influenced by the presence of reactive oxygen species like H_2O_2 (Gomes et al., 2005).

5.1.1 Key signalling pathways involved.

5.1.1.1 NF-κB pathway. TNF-alpha and H_2O_2 can activate the NF-κB pathway, crucial for IL-6 production. NF-κB activation through degradation of IκB allows transcription of inflammatory cytokines, including IL-6 (Schreck et al., 1991). Investigating the pathway using inhibitors like BAY 11-7082 could clarify its regulatory role.

5.1.1.2 JAK/STAT pathway. IL-10 production is often mediated via the JAK/STAT pathway, particularly STAT3, which is activated by H_2O_2 and TNF-alpha as a compensatory mechanism (Aggarwal et al., 2002). STAT3 inhibitors could be used to assess the impact on IL-10 regulation.

5.1.1.3 MAPK pathway. This pathway regulates both pro-inflammatory (IL-6) and anti-inflammatory (IL-10) cytokines. The activation of ERK, JNK, and p38 MAPKs by TNF-alpha and H_2O_2 suggests their involvement in cytokine expression (Nathan & Ding, 2010). Specific inhibitors like SB203580 (p38) and SP600125 (JNK) can be employed to explore their roles.

5.1.1.4 Oxidative stress pathways (Nrf2 & AP-1). H_2O_2 activates oxidative stress pathways, including Nrf2 and AP-1, which can regulate both IL-6 and IL-10 expression (Gomes et al., 2005). Nrf2 activators or inhibitors could be explored to see how oxidative stress impacts cytokine regulation.

5.1.2 Experimental follow-up suggestions.

5.1.2.1 Dose-response and time-course studies. Analysing different concentrations of H_2O_2 and TNF-alpha would help determine the threshold and timing of cytokine responses.

5.1.2.2 Inhibition studies. Blocking NF-κB, JAK/STAT, and MAPK pathways using specific inhibitors (e.g., Stattic for STAT3, SB203580 for p38) could help confirm the pathways involved in cytokine production.

5.1.2.3 Antioxidant studies. Introducing antioxidants like N-acetyl cysteine (NAC) to neutralize oxidative stress would clarify the role of oxidative stress in cytokine expression (Gomes et al., 2005).

5.1.2.4 Gene silencing experiments. Silencing key signalling proteins using siRNA or CRISPR could provide direct evidence of their involvement in cytokine regulation (Szatrowski & Nathan, 1991).

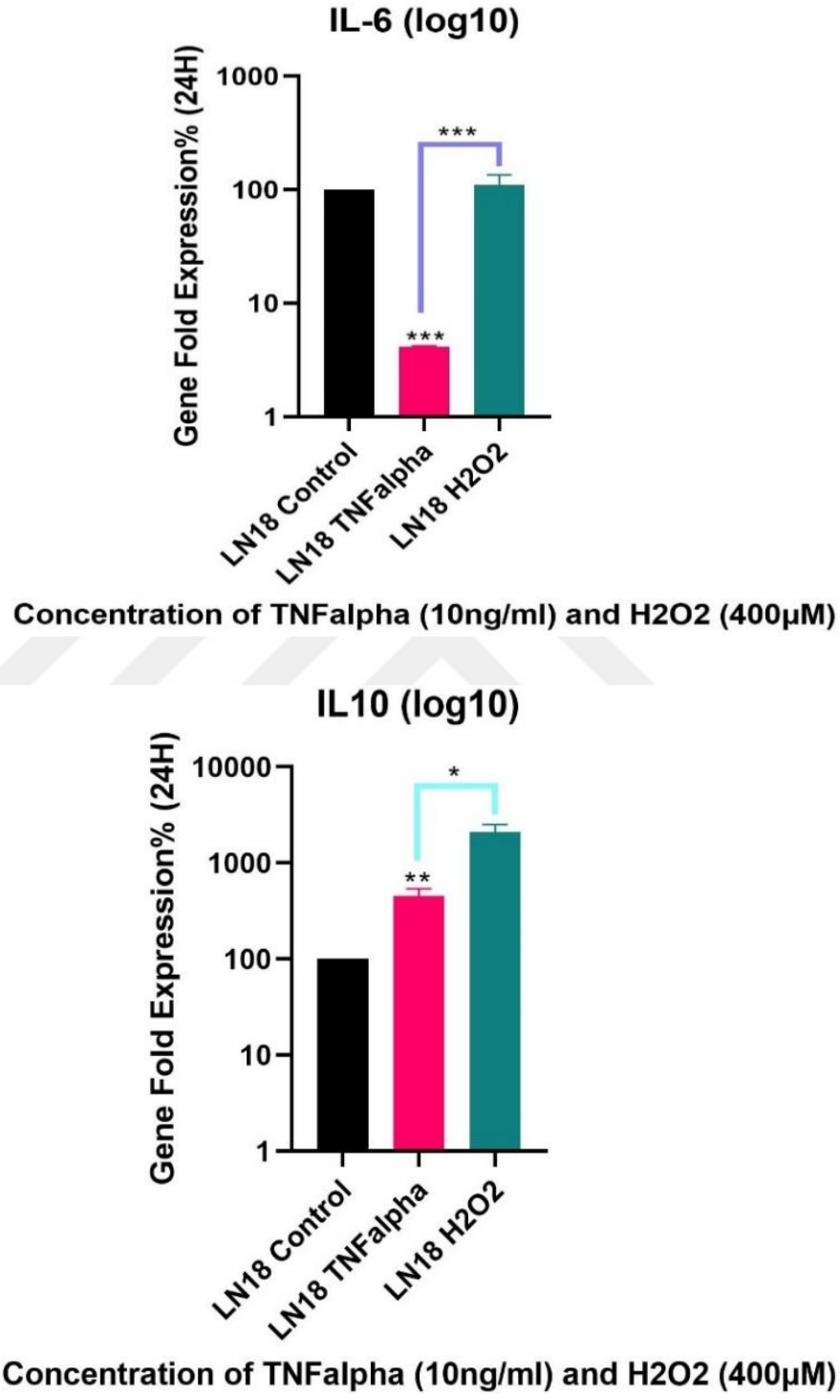

Figure 34. qRT-PCR gene fold expressions of IL-6 and IL-10 of LN18 in 24 hours. Analysis was done by one-way ANOVA, **** $p < 0.0001$, *** $p < 0.001$, ** $p < 0.01$, * $p < 0.05$.

TNF-alpha treatment leads to a suppression of IL-6 expression, which is unexpected given that TNF-alpha is typically known to upregulate pro-inflammatory cytokines (Aggarwal et al., 2002). This could indicate that in LN18 cells, TNF-alpha might trigger a unique feedback mechanism that inhibits IL-6 production.

H_2O_2 treatment, on the other hand, dramatically increases IL-6 expression, consistent with the role of oxidative stress in promoting inflammation through pathways such as NF-κB and MAPK (Schreck et al., 1991).

Both TNF-alpha and H_2O_2 treatments result in an increase in IL-10 expression. The increase in IL-10 under oxidative stress (H_2O_2) is likely a compensatory anti-inflammatory mechanism, as IL-10 functions to limit excessive inflammatory responses (Cavaillon, 2001). This suggests that even in a highly inflammatory environment (due to H_2O_2 -induced oxidative stress), LN18 cells may activate an anti-inflammatory response through IL-10 to maintain homeostasis.

The reduction in IL-6 expression after TNF-alpha treatment is unusual. Further studies could explore the pathways involved, particularly looking at whether the JAK/STAT pathway, which is more often associated with anti-inflammatory responses, plays a role in this observation (Aggarwal et al., 2002). Using inhibitors like tofacitinib (JAK inhibitor) could provide insights into how TNF-alpha downregulates IL-6.

The fact that H_2O_2 induces both IL-6 and IL-10 indicates a dual pro-inflammatory and compensatory anti-inflammatory response. This is consistent with studies showing that oxidative stress can trigger both inflammation and protective responses (Gomes et al., 2005). Future studies could investigate the balance between pro- and anti-inflammatory signalling under oxidative stress by inhibiting NF-κB and analysing the downstream effects on IL-6 and IL-10.

Given the different behaviors of TNF-alpha and H_2O_2, performing time-course experiments could help clarify when each cytokine peaks and how the expression dynamics evolve over time. This would give insights into the temporal regulation of inflammation and resolution in LN18 cells.

Introducing antioxidants like N-acetylcysteine (NAC) could help determine if reducing oxidative stress alters the IL-6/IL-10 balance, particularly focusing on whether oxidative stress is the main driver of IL-6 upregulation and IL-10 compensatory responses.

The LN18 cell line shows interesting patterns of cytokine regulation, with TNF-alpha downregulating IL-6 and upregulating IL-10, while H_2O_2 enhances both IL-6 and IL-10 expression. Targeting specific pathways like NF-κB and JAK/STAT, and performing antioxidant experiments, could provide deeper insights into the inflammatory and compensatory anti-inflammatory responses in these cells.

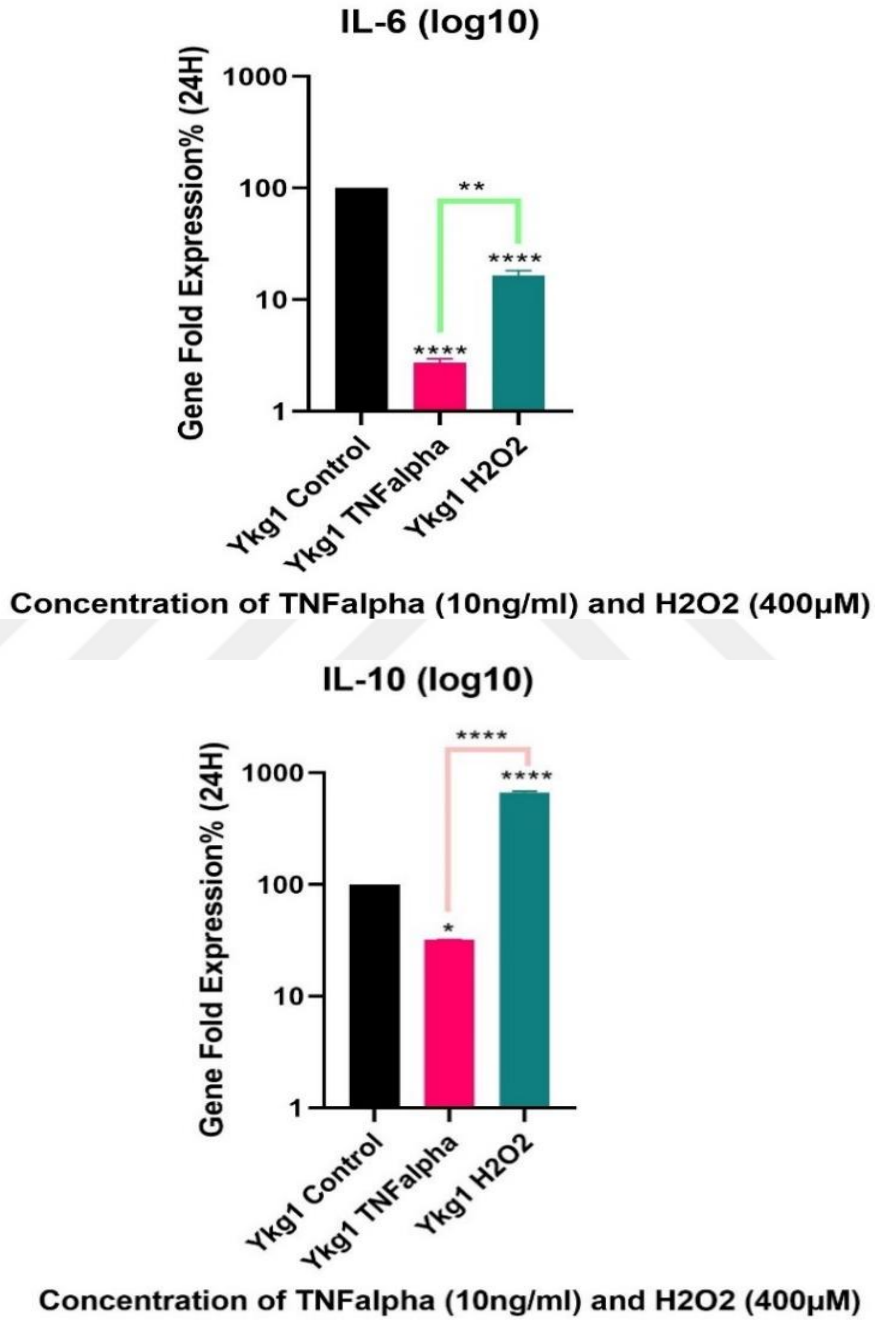

Figure 35. qRT-PCR gene fold expressions of IL-6 and IL-10 of YKG1 in 24 hours. Analysis was done by one-way ANOVA, **** $p < 0.0001$, *** $p < 0.001$, ** $p < 0.01$, * $p < 0.05$.

NF-alpha treatment leads to a decrease in IL-6 expression, which is atypical since TNF-alpha is generally known to promote IL-6 production in inflammatory conditions (Aggarwal et al., 2002). This suggests that TNF-alpha might be triggering a negative feedback loop or a pathway that suppresses pro-inflammatory responses in Ykg1 cells.

H_2O_2 treatment causes a significant increase in IL-6 expression, though still not as high as in the control group. This indicates that oxidative stress from H_2O_2 induces an inflammatory response, though not as strongly as in other cell lines like LN18. The involvement of oxidative stress pathways, such as NF-κB and AP-1, may explain this increase (Schreck et al., 1991).

Both TNF-alpha and H_2O_2 induce IL-10 expression, with H_2O_2 showing a much stronger effect. IL-10 is an anti-inflammatory cytokine, and its upregulation, particularly under oxidative stress, suggests that Ykg1 cells are actively working to counterbalance inflammation. This could involve activation of the JAK/STAT3 pathway, which is known to mediate IL-10 production (Cavaillon, 2001).

The suppression of IL-6 by TNF-alpha in Ykg1 cells suggests an unusual regulatory mechanism. Future experiments could focus on the JAK/STAT pathway, potentially involving STAT3 or SOCS (Suppressor of Cytokine Signalling) proteins, which could inhibit IL-6 production. Inhibitors like Stattic (STAT3 inhibitor) can be used to explore these pathways further (Aggarwal et al., 2002).

The relatively modest increase in IL-6 under H_2O_2 treatment suggests that oxidative stress activates inflammatory pathways but does not induce an overwhelming pro-inflammatory response in Ykg1 cells. This could be explored further by using antioxidants like N-acetyl cysteine (NAC) to see if reducing oxidative stress lowers IL-6 levels. Additionally, exploring the involvement of NF-κB using inhibitors (e.g., BAY 11-7082) could help understand how oxidative stress drives IL-6 expression (Schreck et al., 1991).

The significant increase in IL-10, particularly under H_2O_2, indicates a strong compensatory response to oxidative stress. Investigating whether this increase is sufficient to dampen the inflammatory effects of IL-6 could be crucial. Using STAT3 inhibitors or siRNA to knock down IL-10 expression could help assess whether the anti-inflammatory response is mediated through this pathway (Cavaillon, 2001).

Conducting time-course experiments to monitor how IL-6 and IL-10 levels change over time in response to TNF-alpha and H_2O_2 would provide insights into the temporal dynamics of pro- and anti-inflammatory responses. A dose-response study varying the concentrations of H_2O_2 and TNF-alpha could further clarify the threshold for triggering significant cytokine changes.

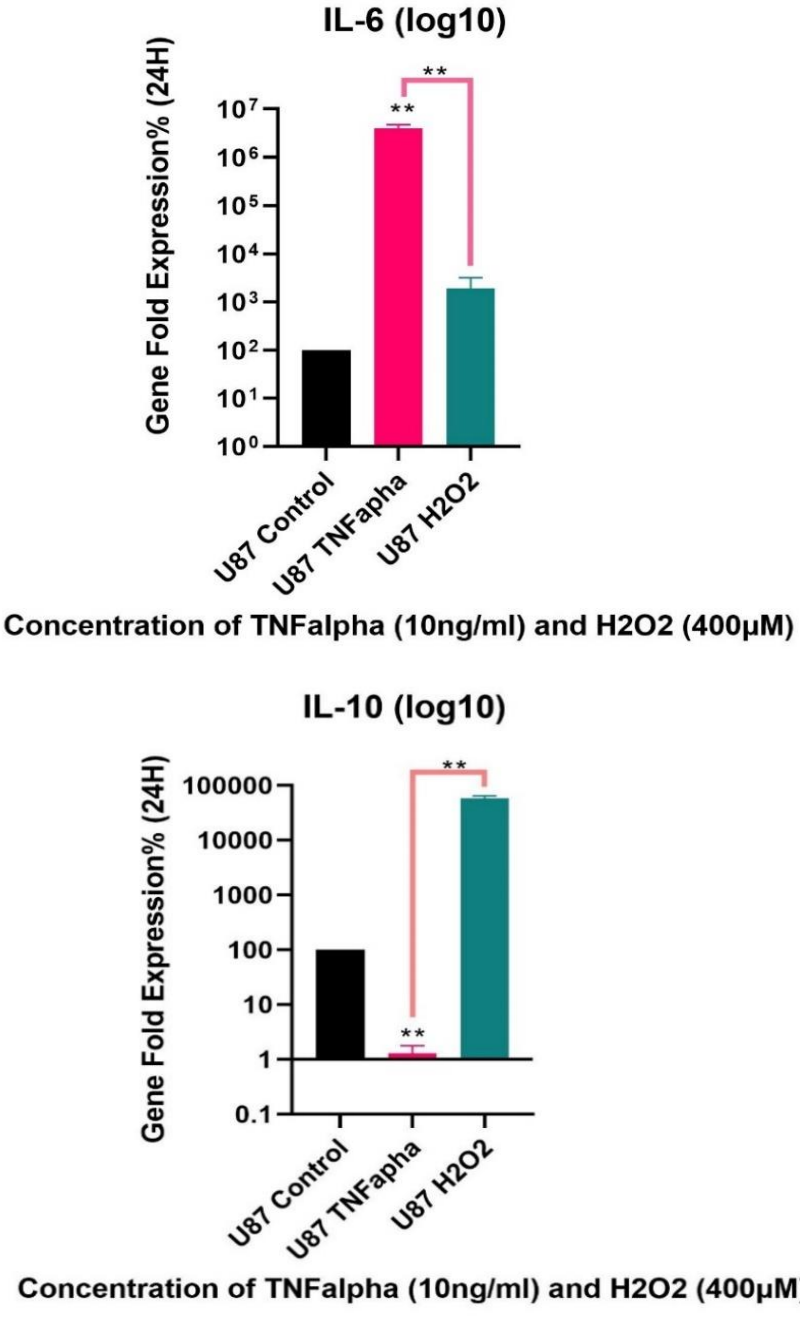

Figure 36. qRT-PCR gene fold expressions of IL-6 and IL-10 of U87 in 24 hours. Analysis was done by one-way ANOVA, **** $p < 0.0001$, *** $p < 0.001$, ** $p < 0.01$, * $p < 0.05$.

TNF-alpha induces a dramatic increase in IL-6 expression, which is expected as TNF-alpha is a well-known activator of inflammatory pathways such as NF-κB (Aggarwal et al., 2002). This result suggests that TNF-alpha strongly activates the pro-inflammatory signalling in U87 cells.

H_2O_2 also increases IL-6 expression, but to a lesser extent. This is consistent with oxidative stress activating NF-κB and other pro-inflammatory pathways like AP-1, though the response is less intense than with TNF-alpha (Schreck et al., 1991).

TNF-alpha treatment leads to a reduction in IL-10 expression, indicating a suppression of anti-inflammatory signalling. This suggests that the pro-inflammatory environment created by TNF-alpha in U87 cells may inhibit pathways like JAK/STAT3, which are typically involved in IL-10 production (Cavaillon, 2001).

H_2O_2, however, induces a massive increase in IL-10 expression, likely as a compensatory response to oxidative stress. The strong upregulation of IL-10 may be an attempt by U87 cells to counterbalance the inflammatory effects of IL-6, which is consistent with the activation of STAT3 by oxidative stress (Nathan & Ding, 2010).

The large increase in IL-6 after TNF-alpha treatment suggests strong activation of the NF-κB pathway. Using NF-κB inhibitors (e.g., BAY 11-7082) could help determine whether this pathway is the primary driver of IL-6 upregulation in U87 cells (Schreck et al., 1991). Exploring the role of MAPK (especially p38 MAPK) might also be useful since it is another pathway involved in IL-6 production.

The suppression of IL-10 by TNF-alpha is unusual and suggests a possible inhibition of JAK/STAT3 signalling in U87 cells. This can be further explored by using STAT3 inhibitors or siRNA to knockdown STAT3 expression and evaluate the changes in IL-10 production (Cavaillon, 2001).

The dramatic increase in IL-10 following H_2O_2 treatment suggests a protective or compensatory anti-inflammatory response. Investigating the involvement of Nrf2 and STAT3 pathways, both of which are activated by oxidative stress, could provide insights into the mechanisms regulating IL-10 (Gomes et al., 2005). Antioxidants like N-acetyl cysteine (NAC) could be used to explore whether reducing oxidative stress impacts IL-10 expression.

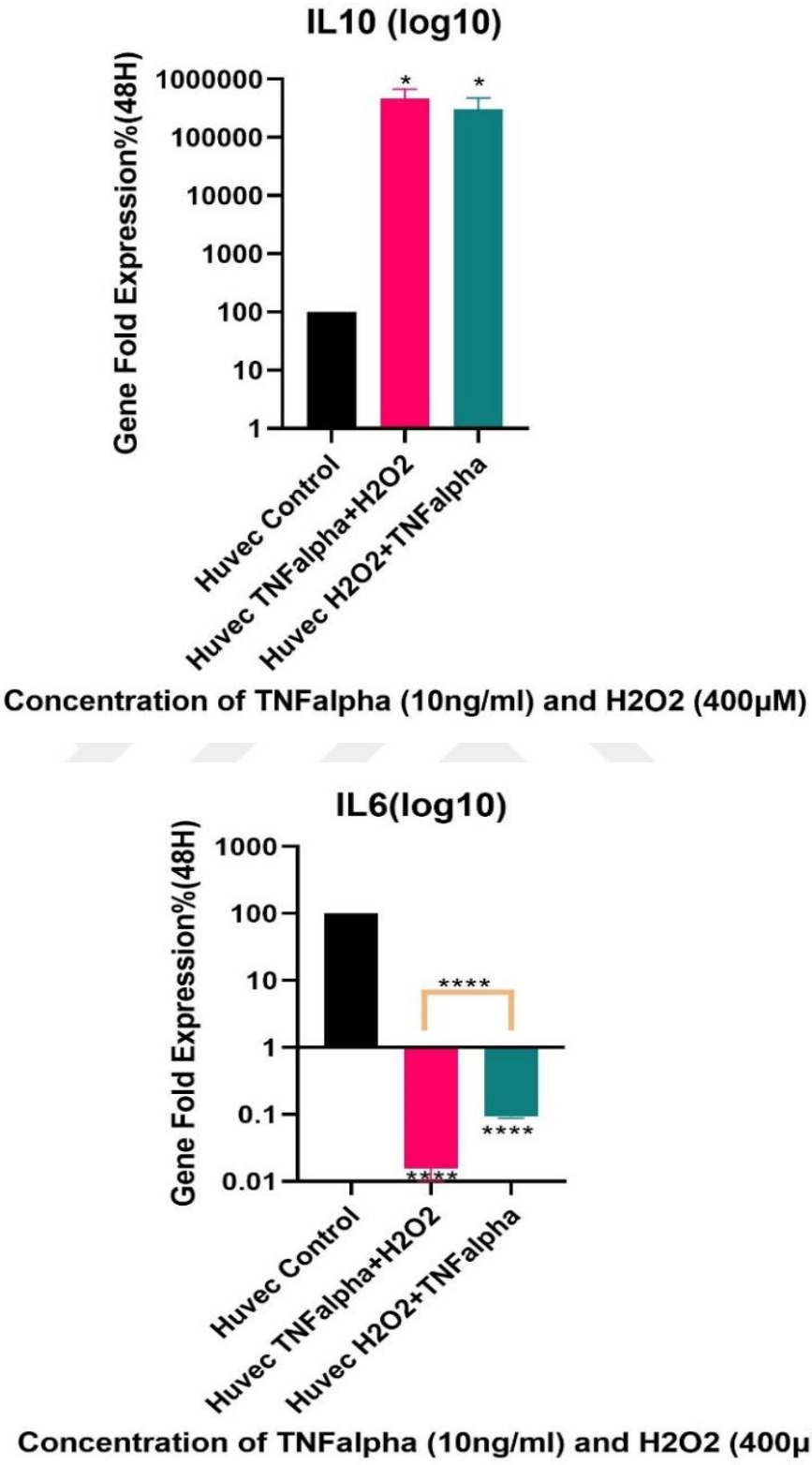

Figure 37. qRT-PCR gene fold expressions of IL-10 and IL-6 of HUVEC in 48 hours. Analysis was done by one-way ANOVA, **** $p < 0.0001$, *** $p < 0.001$, ** $p < 0.01$, * $p < 0.05$.

Both combinations of TNF-alpha + H_2O_2 and H_2O_2 + TNF-alpha treatments lead to a dramatic increase in IL-10 expression. This suggests that the cells are mounting a strong anti-inflammatory response to counteract the pro-inflammatory effects of both TNF-alpha and oxidative stress from H_2O_2. The near-identical levels of IL-10 indicate that both orderings of treatment have a similar impact on IL-10 upregulation (Cavaillon, 2001).

Both TNF-alpha + H_2O_2 and H_2O_2 + TNF-alpha treatments result in a significant suppression of IL-6 expression, with values dropping well below the control level. This suggests that in HUVEC cells, the combination of TNF-alpha and H_2O_2 may inhibit pro-inflammatory pathways, perhaps through feedback inhibition or activation of negative regulators like SOCS (Suppressor of Cytokine Signalling) (Aggarwal et al., 2002).

The significant suppression of IL-6 by both TNF-alpha and H_2O_2 combinations in HUVEC cells is unexpected given the typical role of TNF-alpha as an activator of IL-6. This suggests a possible involvement of negative feedback mechanisms or anti-inflammatory pathways that dampen IL-6 production. Investigating the role of SOCS proteins or the activation of Nrf2 signalling (related to oxidative stress) could provide insights (Aggarwal et al., 2002; Gomes et al., 2005).

The robust increase in IL-10 expression in response to both treatment combinations suggests that HUVEC cells are activating compensatory anti-inflammatory pathways to counterbalance oxidative and inflammatory stress. This strong IL-10 response likely involves the JAK/STAT3 pathway (Cavaillon, 2001). Further experiments using STAT3 inhibitors could determine the importance of this pathway in regulating IL-10 expression under stress conditions.

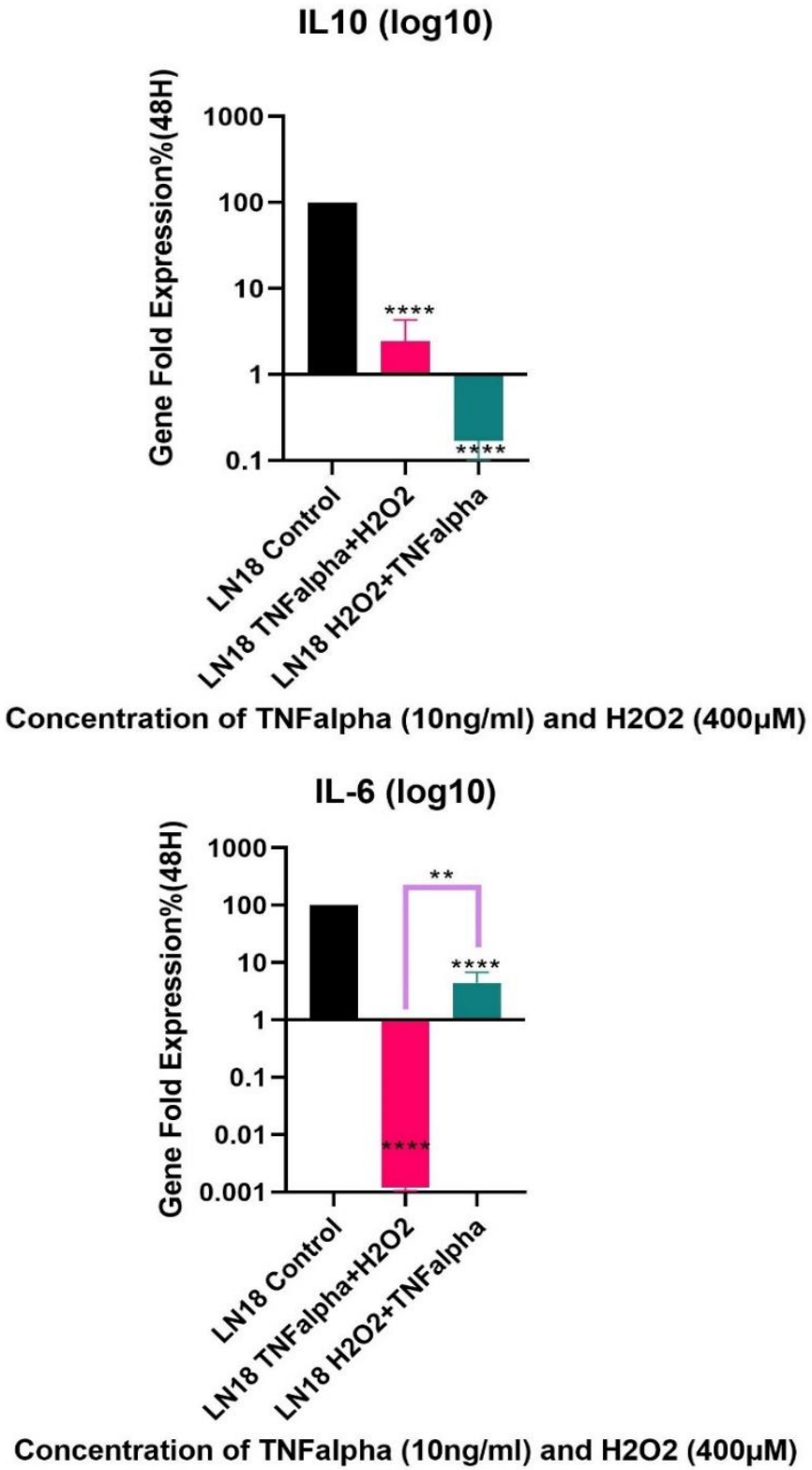

Figure 38. qRT-PCR gene fold expressions of IL-10 and IL-6 of LN18 in 48 hours. Analysis was done by one-way ANOVA, **** $p < 0.0001$, *** $p < 0.001$, ** $p < 0.01$, * $p < 0.05$.

Both treatment combinations significantly suppress IL-10 expression in LN18 cells. This indicates that oxidative stress (H_2O_2) combined with TNF-alpha leads to a marked suppression of anti-inflammatory responses, possibly through inhibition of the JAK/STAT3 pathway, which is typically responsible for IL-10 production (Cavaillon, 2001). The greater suppression in the H_2O_2 + TNF-alpha combination suggests that the sequence of treatment might affect the anti-inflammatory response.

The significant suppression of IL-6 expression in both treatments suggests that, unlike in other cell types, LN18 cells respond to oxidative stress and inflammatory signals by suppressing the pro-inflammatory cytokine. This is surprising, as TNF-alpha is generally expected to upregulate IL-6 through NF-κB and AP-1 pathways (Aggarwal et al., 2002). The slight recovery in the H_2O_2 + TNF-alpha treatment suggests that this combination might induce a weak compensatory response, though still much lower than control levels.

The strong suppression of IL-10 by both treatment combinations suggests inhibition of anti-inflammatory signalling pathways like JAK/STAT3. Future experiments could investigate whether this suppression is mediated by negative feedback inhibitors like SOCS (Suppressor of Cytokine Signalling) or whether oxidative stress specifically downregulates IL-10 production in LN18 cells (Cavaillon, 2001). STAT3 inhibitors could be used to explore the pathway in more detail.

The suppression of IL-6 in both treatments is unexpected given TNF-alpha's usual role in promoting IL-6 via NF-κB activation (Aggarwal et al., 2002). Investigating whether negative feedback loops, such as the activation of Nrf2 in response to oxidative stress, contribute to this suppression could provide useful insights. NF-κB inhibitors could be applied to determine the role of this pathway in IL-6 regulation.

Given the strong suppression of both IL-6 and IL-10, exploring whether antioxidants (e.g., N-acetyl cysteine) or anti-inflammatory drugs could restore the balance between these cytokines may be useful. These treatments could help determine whether oxidative stress is the primary driver of cytokine suppression in LN18 cells (Gomes et al., 2005).

.

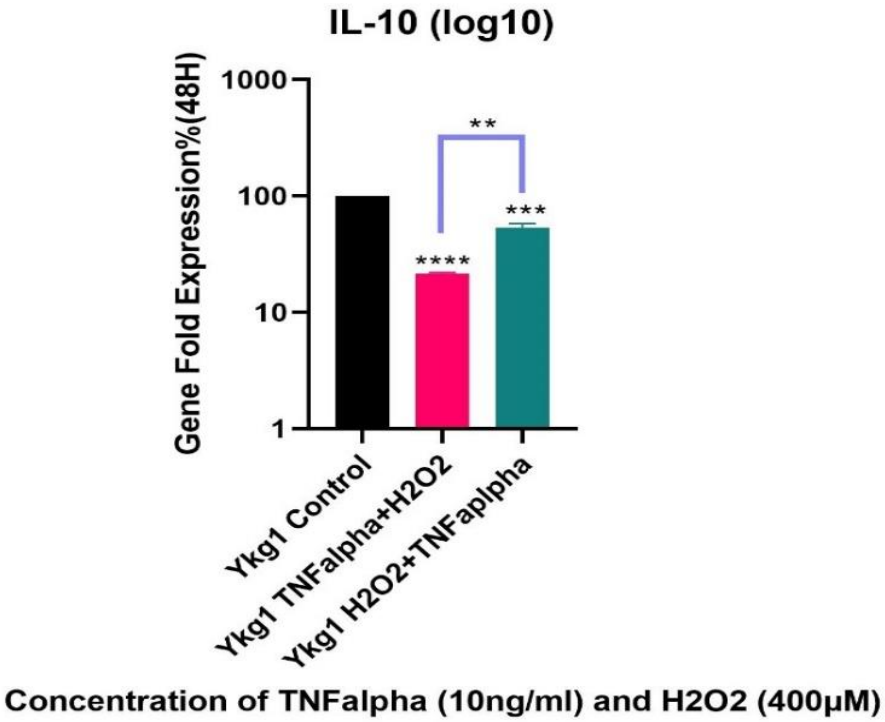

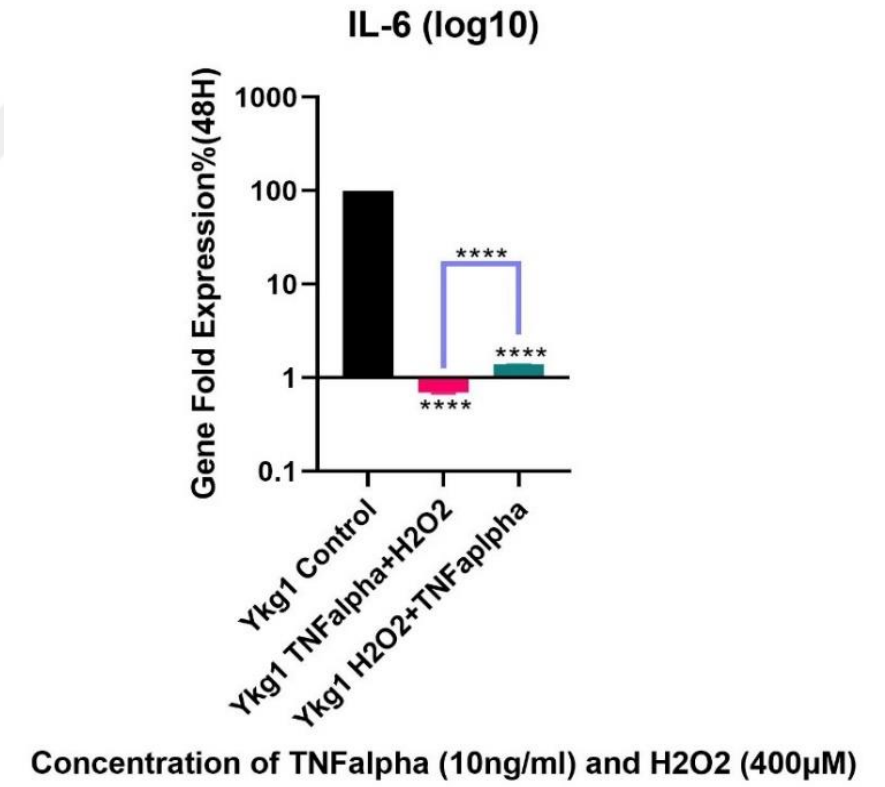

Figure 39. qRT-PCR gene fold expressions of IL-10 and IL-6 of YKG1 in 48 hours. Analysis was done by one-way ANOVA, **** $p < 0.0001$, *** $p < 0.001$, ** $p < 0.01$, * $p < 0.05$.

The combination of TNF-alpha and H_2O_2 significantly suppresses IL-10 expression, indicating a reduced anti-inflammatory response. The slight recovery seen in the H_2O_2 + TNF-alpha treatment group suggests that the order of treatment might affect the degree of suppression, with oxidative stress possibly mitigating TNF-alpha's inhibitory effect on IL-10 (Cavaillon, 2001).

Both treatments significantly suppress IL-6 expression in Ykg1 cells, suggesting that the combined effect of TNF-alpha and oxidative stress (H_2O_2) leads to a marked suppression of pro-inflammatory signalling. This suppression may involve negative feedback mechanisms, such as SOCS proteins or oxidative stress-induced pathways like Nrf2 that counteract pro-inflammatory signals (Aggarwal et al., 2002; Gomes et al., 2005).

The suppression of IL-10 in both treatment groups indicates inhibition of anti-inflammatory pathways, possibly through the downregulation of the JAK/STAT3 pathway (Cavaillon, 2001). Further studies should investigate whether oxidative stress from H_2O_2 combined with TNF-alpha triggers negative feedback mechanisms like SOCS that inhibit IL-10 production.

The unexpected suppression of IL-6, a typical marker of inflammation, suggests that the NF-κB pathway, which is usually activated by TNF-alpha, might be inhibited under these conditions (Aggarwal et al., 2002). Investigating whether Nrf2 or other oxidative stress-response pathways are activated could reveal how the suppression occurs. NF-κB inhibitors (such as BAY 11-7082) could be used to further investigate whether IL-6 suppression is related to feedback loops.

The suppression of both IL-6 and IL-10 suggests a dampening of both pro- and anti-inflammatory responses. Future studies could assess whether interventions with antioxidants (e.g., N-acetyl cysteine) or anti-inflammatory agents could restore IL-10 levels without suppressing IL-6, thereby promoting a more balanced immune response in Ykg1 cells (Nathan & Ding, 2010).

Time-course experiments could help determine when the suppression of IL-6 and IL-10 begins after TNF-alpha and H_2O_2 treatment. This would clarify whether the suppression is an early or late event and could guide therapeutic interventions aimed at preventing or reversing this suppression.

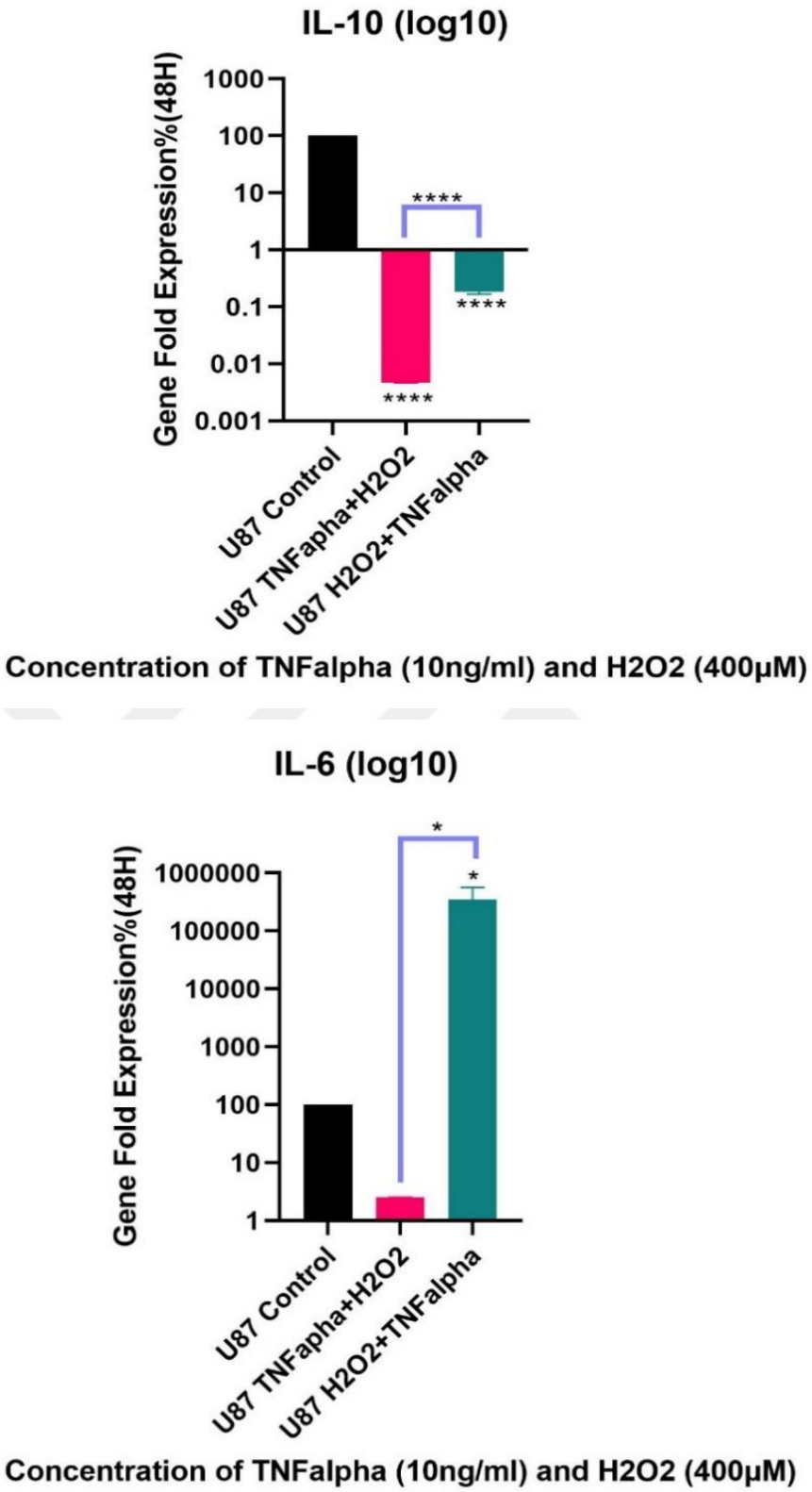

Figure 40. qRT-PCR gene fold expressions of IL-10 and IL-6 of U87 in 48 hours. Analysis was done by one-way ANOVA, **** $p < 0.0001$, *** $p < 0.001$, ** $p < 0.01$, * $p < 0.05$.

Both treatments significantly suppress IL-10 expression in U87 cells, indicating a dampened anti-inflammatory response under the combined influence of TNF-alpha and H_2O_2. The slight recovery seen in the H_2O_2 + TNF-alpha group may suggest that oxidative stress induces a partial reversal of the TNF-alpha-driven suppression of IL-10 (Cavaillon, 2001). This could imply a context-dependent modulation of anti-inflammatory pathways such as JAK/STAT3, which typically drives IL-10 expression.

TNF-alpha + H_2O_2 strongly suppresses IL-6 production, suggesting an unexpected reduction of the pro-inflammatory response in U87 cells under these conditions. However, the H_2O_2 + TNF-alpha treatment shows an extreme upregulation of IL-6, indicating a highly inflammatory environment when oxidative stress precedes TNF-alpha stimulation. This suggests that the order of exposure to these stressors critically influences the inflammatory outcome, likely through pathways like NF-κB (Aggarwal et al., 2002).

The suppression of IL-10 in both treatment groups points to the inhibition of JAK/STAT3 signalling, which is typically responsible for driving IL-10 expression (Cavaillon, 2001). Further studies could explore whether SOCS proteins or other feedback inhibitors are involved in this suppression, and whether oxidative stress modulates these pathways in a context-dependent manner.

The extreme upregulation of IL-6 in the H_2O_2 + TNF-alpha group suggests a powerful activation of the NF-κB and/or AP-1 pathways, which are known to be involved in pro-inflammatory responses to oxidative stress (Schreck et al., 1991). NF-κB inhibitors like BAY 11-7082 could be applied to dissect whether this pathway is driving the IL-6 surge in response to combined oxidative stress and TNF-alpha exposure.

Given the significant upregulation of IL-6, particularly in the H_2O_2 + TNF-alpha group, therapeutic interventions aimed at balancing the pro- and anti-inflammatory responses could be explored. Using antioxidants like N-acetyl cysteine (NAC) to reduce oxidative stress or anti-inflammatory drugs targeting NF-κB could help restore the balance between IL-6 and IL-10 in U87 cells (Nathan & Ding, 2010).

5.2 Conclusion

The analysis of IL-6 and IL-10 gene expression in various cell lines under combined TNF-alpha and H_2O_2 treatments reveals important insights:

Differential Responses: Glioblastoma cell lines (U87, Ykg1, LN18) and HUVEC cells exhibit distinct pro-inflammatory and anti-inflammatory cytokine responses to the same treatments. U87 cells display an exaggerated inflammatory response, while Ykg1 and LN18 cells suppress both pro- and anti-inflammatory signals.

Impact of Treatment Order: The order in which TNF-alpha and H_2O_2 are applied significantly affects cytokine expression. Oxidative stress preceding inflammatory stimulation exacerbates IL-6 expression in U87 cells, indicating a priming effect that heightens inflammation.

Therapeutic Implications: The broad suppression of IL-10 suggests that combined oxidative and inflammatory stress could impair anti-inflammatory responses, potentially leading to chronic inflammation or disease progression. Therapeutic strategies targeting oxidative stress and inflammation, particularly by modulating pathways like NF-κB and JAK/STAT3, may help restore balance between IL-6 and IL-10, reducing inflammation while promoting appropriate immune regulation.

Targeting Inflammatory Pathways: In U87 cells, where IL-6 upregulation is extreme, NF-κB inhibitors could be explored to mitigate excessive inflammation. Additionally, boosting Nrf2 activation or antioxidant responses may help reduce oxidative stress-induced cytokine imbalances.

Restoring IL-10 Function: Further research into JAK/STAT3 pathway modulation could help restore IL-10 expression in glioblastoma cell lines, potentially preventing chronic inflammation and creating an environment less conducive to tumor progression.

Context-Specific Treatments: Given the variability in responses across cell types, tailored approaches targeting both inflammation and oxidative stress could be essential for effective treatment strategies in diseases characterized by inflammatory and oxidative stress, such as cancer and neuroinflammation.

REFERENCES

Aggarwal, B. B. (2003). Signaling pathways of the TNF superfamily: a double-edged sword. Nature Reviews Immunology, 3(9), 745-756.

Balkwill, F. (2009). Tumour necrosis factor and cancer. Nature Reviews Cancer, 9(5), 361-371.

BioRender. (n.d.). *BioRender: Science made simple*. https://www.biorender.com/

Cancer Genome Atlas Research Network. (2008). Comprehensive genomic characterization defines human glioblastoma genes and core pathways. Nature, 455(7216), 1061-1068.

Cavaillon, J. M. (2001). Pro- versus anti-inflammatory cytokines: Myth or reality. *Cellular and Molecular Biology*, *47*(4), 695-702.

Couper, K. N., Blount, D. G., & Riley, E. M. (2008). IL-10: the master regulator of immunity to infection. Journal of Immunology, 180(9), 5771-5777.

Fiorentino, D. F., Zlotnik, A., Mosmann, T. R., Howard, M., & O'Garra, A. (1991). IL-10 inhibits cytokine production by activated macrophages. *Journal of Immunology, 147*(11), 3815-3822

Fulda, S. (2009). Tumor necrosis factor-related apoptosis-inducing ligand (TRAIL). Advances in Experimental Medicine and Biology, 647, 195-206.

Gomes, A., Fernandes, E., & Lima, J. L. F. C. (2005). Fluorescence probes used for detection of reactive oxygen species. *Journal of Biochemical and Biophysical Methods*, *65*(2–3), 45-80. https://doi.org/10.1016/j.jbbm.2005.10.003

Gorrini, C., Harris, I. S., & Mak, T. W. (2013). Modulation of oxidative stress as an anticancer strategy. Nature Reviews Drug Discovery, 12(12), 931-947.

Gosset, P., Wallaert, B., Tonnel, A. B., & Joseph, M. (1993). Increased secretion of tumor necrosis factor-alpha, interleukin-6, interleukin-8, and interleukin-10 by alveolar macrophages from patients with acute respiratory distress syndrome. *American Journal of Respiratory and Critical Care Medicine, 148*(2), 340-346.

Guo, L., Xu, J., Qi, J., & Zhang, L. (2018). microRNA-132-3p inhibits glioma cell proliferation, invasion and migration by targeting SOX9. OncoTargets and Therapy, 11, 7593-7601.

Gurgul, I., Janczy-cempa, E., Gajda-morszewski, P., & Mazuryk, O. (2022). Moving Ru polypyridyl complexes beyond cytotoxic activity towards metastasis inhibition, *226*. https://doi.org/10.1016/j.jinorgbio.2021.111652

Huang, S., Guo, W., Tang, Y., Ren, D., Zou, X., Peng, X., ... & Zhang, X. (2016). miR-342-3p inhibits cell proliferation and invasion by targeting AKT1 in hepatocellular carcinoma. Journal of Cell Science, 129(7), 1365-1373.

Inda, M. M., Bonavia, R., Mukasa, A., Narita, Y., Sah, D. W., Vandenberg, S., ... & Cavenee, W. K. (2010). Tumor heterogeneity is an active process maintained by a mutant EGFR-induced cytokine circuit in glioblastoma. Genes & Development, 24(16), 1731-1745.

Kanzawa, T., Germano, I. M., Komata, T., Ito, H., Kondo, Y., & Kondo, S. (2003). Role of autophagy in temozolomide-induced cytotoxicity for malignant glioma cells. Cell Death and Differentiation, 10(2), 136-142.

Kishimoto, T. (2006). Interleukin-6: discovery of a pleiotropic cytokine. Arthritis Research & Therapy, 8(Suppl 2), S2.

Liang, L., Gu, Y., Tang, Y., & Zhang, X. (2015). miR-193b-5p suppresses cell proliferation and invasion by targeting MCL1 in cervical cancer. OncoTargets and Therapy, 8, 6157-6164.

Libby, P., Ridker, P. M., & Maseri, A. (2002). Inflammation and atherosclerosis. *Circulation*, *105*(9), 1135-1143. https://doi.org/10.1161/hc0902.104353

Louis, D. N., Perry, A., Reifenberger, G., von Deimling, A., Figarella-Branger, D., Cavenee, W. K., ... & Ellison, D. W. (2016). The 2016 World Health Organization classification of tumors of the central nervous system: a summary. Acta Neuropathologica, 131(6), 803-820.

Morgan, M. J., & Liu, Z. G. (2011). Crosstalk of reactive oxygen species and NF-κB signaling. Cell Research, 21(1), 103-115.

Mosmann, T. (1983). Rapid colorimetric assay for cellular growth and survival: application to proliferation and cytotoxicity assays. Journal of Immunological Methods, 65(1-2), 55-63.

Nathan, C., & Ding, A. (2010). Nonresolving inflammation. *Cell*, *140*(6), 871-882. https://doi.org/10.1016/j.cell.2010.02.029

Nucleogene. (n.d.). Nucleic acid extraction kits. https://www.nucleogene.com/product-nucleogene-nucleic-acid-extraction-kits

Schieber, M., & Chandel, N. S. (2014). ROS function in redox signaling and oxidative stress. Current Biology, 24(10), R453-R462.

Schreck, R., Rieber, P., & Baeuerle, P. A. (1991). Reactive oxygen intermediates as apparently widely used messengers in the activation of the NF-κB transcription factor and HIV-1. *The EMBO Journal*, *10*(8), 2247-2258.

Sosa, V., Moliné, T., Somoza, R., Paciucci, R., Kondoh, H., & LLeonart, M. E. (2013). Oxidative stress and cancer: an overview. Ageing Research Reviews, 12(1), 376-390.

Stupp, R., Hegi, M. E., Mason, W. P., van den Bent, M. J., Taphoorn, M. J., Janzer, R. C., ... & Mirimanoff, R. O. (2005). Effects of radiotherapy with concomitant and adjuvant temozolomide versus radiotherapy alone on survival in glioblastoma. New England Journal of Medicine, 352(10), 987-996.

Szatrowski, T. P., & Nathan, C. F. (1991). Production of large amounts of hydrogen peroxide by human tumor cells. *Cancer Research*, *51*(3), 794-798.

Trachootham, D., Lu, W., Ogasawara, M. A., Nilsa, R. D., & Huang, P. (2009). Redox regulation of cell survival. Antioxidants & Redox Signaling, 10(8), 1343-1374.

Van Horssen, R., Ten Hagen, T. L., & Eggermont, A. M. (2006). TNF-α in cancer treatment: molecular insights, antitumor effects, and clinical utility. The Oncologist, 11(4), 397-408.

Wajant, H., Pfizenmaier, K., & Scheurich, P. (2003). Tumor necrosis factor signaling. Cell Death and Differentiation, 10(1), 45-65.

Wang, X., Yousefi, S., & Simon, H. U. (2008). Necroptosis and neutrophil-associated disorders. Cell Death & Differentiation, 15(5), 728-736.

Wang, Y., Xie, Y., Zhang, A., Wang, M., Fang, Z., & Shen, C. (2017). miR-342-3p inhibits proliferation and invasion of colorectal cancer cells by targeting BCL2-associated athanogene 3. Medical Science Monitor, 23, 5869-5876.

Wu, L., Cai, C., Wang, X., Liu, M., & Li, X. (2015). miR-132-3p inhibits cell proliferation and invasion by targeting SOX9 in human non-small cell lung cancer. Journal of Experimental & Clinical Cancer Research, 34(1), 146.

Xu, X., Jia, R., Zhou, Y., Song, X., Wang, J., Qian, G., ... & Liang, X. (2016). Microarray-based analysis: Identification of hypoxia-regulated microRNAs in retinoblastoma cells. International Journal of Oncology, 49(6), 2361-2370.

Yamanaka, R., Hayano, A., Kanayama, T., Arai, H., & Tanaka, R. (2001). In vitro chemosensitivity of malignant glioma cell lines using the MTT assay. Journal of Neuro-Oncology, 53(2), 149-158.

Zhu, Y., Parada, L. F., & Cooper, G. M. (2012). GABPα and GABPβ: molecular links between growth factor signaling and oncogenesis. Oncogene, 21(21), 3293-3301.